

THE UNIVERSITY OF MICHIGAN
ANN ARBOR, MICHIGAN

INTERIM SCIENTIFIC REPORT NO. 1

FOR

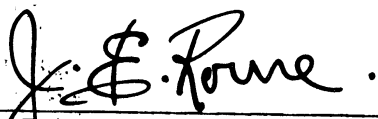
SOLID-STATE MICROWAVE RESEARCH

This report covers the period September 16, 1963 to February 1, 1964

Electron Physics Laboratory
Department of Electrical Engineering

By: D. C. Hanson
J. E. King
J. E. Rowe
C. Yeh

Approved by:



J. E. Rowe, Director
Electron Physics Laboratory

Project 06031

Contract No. AF 33(657)-11587
Electronic Technology Division
Air Force Avionics Laboratory
Research and Technology Division
Air Force Systems Command
Wright-Patterson Air Force Base, Ohio

March, 1964

ABSTRACT

The research investigations described herein relate directly to the general nature of microwave interactions in bulk solid-state materials, which is the principal objective of this broad study. The specific research tasks described in this report relate to the generation and/or amplification of coherent electromagnetic radiation in the microwave-optical regime of the spectrum.

In particular the following three subjects are currently under study and discussed in this report.

1. General parametric phonon interactions in solids.
2. Radiation from bulk materials.
3. Traveling-wave phonon interactions.

The general nature of each of these phenomena is outlined in this report and both theoretical and experimental active programs are outlined.

TABLE OF CONTENTS

	<u>Page</u>
ABSTRACT	iii
LIST OF ILLUSTRATIONS	vi
LIST OF TABLES	vii
PERSONNEL	viii
1. GENERAL INTRODUCTION	1
2. PHONON INTERACTION IN SOLIDS	1
2.1 Background	1
2.2 Review of Theory	3
2.3 Theory	9
2.3.1 Parametric Conditions	9
2.3.2 Interaction of Traveling Waves	11
2.3.3 Phonon Paramagnetic Resonance	18
2.3.4 Theoretical Conclusions	22
2.4 Experimental Apparatus	26
2.5 Program for the Next Quarter	29
3. RADIATION FROM SOLIDS	29
3.1 Introduction	29
3.2 Theory of Operation and Experimental Evidence	30
3.2.1 "Electron-Hole Plasma Oscillations" in a Magnetic Field (The "Oscillistor")	30
3.2.2 The "Gunn Radiation Experiment"	33
3.3 Proposed Experiment	39
3.4 Conclusions	39
3.5 Program for the Next Quarter	42
4. TRAVELING-WAVE PHONON INTERACTIONS	42
4.1 Introduction	42
4.2 Literature Survey	43
4.2.1 Fundamental Effects	43

	<u>Page</u>
4.2.2 The Electro Acoustic Effect	43
4.2.3 The Piezoelectric Effect	44
4.2.4 The Magneto Acoustic Effect	46
4.2.5 Related Effects	47
4.3 Experimental Acoustic-Wave Amplifiers	48
4.4 Amplification Theory	49
4.5 The Acoustic Velocity	58
4.6 Conclusions	61
4.7 Program for the Next Quarter	61

LIST OF ILLUSTRATIONS

<u>Figure</u>		<u>Page</u>
2.1	Dispersion Relation Between Elastic Wave Frequency ω and Phase Constant β . Δ is Stop Band Near Spin Resonance Frequency ω .	6
2.2	Dispersion Relation Between Elastic Wave Frequency ω and Phase Constant β with Loss in the Paramagnetic Absorption Near Spin Resonance Frequency ω .	7
2.3	Transmission Line Transducer.	28
3.1	Proposed Mount and Confocal Detector.	40
3.2	Bulk Specimen and Heat Sink.	41
4.1	Normalized Gain (or Attenuation) $(\alpha v_0/\omega)/(e^2/2c\epsilon)$ vs. Frequency $\gamma(\omega/\omega_c)$ for Various Values of the Parameter $k^2\Lambda^2-1$.	56
4.2	Normalized Acoustic Velocity $[(v/v_0) - 1]/(e^2/2c\epsilon)$ vs. Frequency $\gamma(\omega/\omega_c)$ for Various Values of the Parameter $k^2\Lambda^2-1$.	60

LIST OF TABLES

<u>Table</u>		<u>Page</u>
2.1	Coefficients of Sound Absorption for Ions with $S' = 1/2$. $\sigma = A (\nu^4/T) \times 10^{-40} \text{ cm}^{-1}$	22
2.2	Coefficients of Sound Absorption for Ions with $S' > 1/2$. $\sigma = A (\nu^2/T) \times 10^{-19} \text{ cm}^{-1}$	23
2.3	Coefficients of Absorption of Longitudinal Sound Waves in Ethylsulfates of Rare-Earth Ions with an Even Number of Electrons. $\sigma = A (\nu^2/T) \times 10^{-13} \text{ cm}^{-1}$	23
2.4	Coefficients of Absorption of Sound. Rare-Earth Ions with Odd Number of Electrons. $\sigma = A (\nu^4/T) \times 10^{-40} \text{ cm}^{-1}$	24

PERSONNEL

<u>Scientific and Engineering Personnel</u>		<u>Time Worked in</u> <u>Man Months*</u>
J. E. Rowe	Professor	.40
G. I. Haddad	Assistant Professor	.50
W. Rensel	Assistant Research Engineer	.74
D. Hanson	Research Assistants	.44
J. King		1.90
R. Maire		.79
<u>Service Personnel</u>		12.04

* Time Worked is based on 172 hours per month.

INTERIM SCIENTIFIC REPORT NO. 1

FOR

SOLID-STATE MICROWAVE RESEARCH

1. General Introduction (J. E. Rowe)

The purpose of this research study is to investigate the general characteristics of high-frequency (microwave) interactions in bulk semiconductors. The program is a general one concerned with the generation, amplification and detection of coherent electromagnetic energy in the centimeter through optical regions of the electromagnetic spectrum.

Although the general areas of study under this program cover a wide range of topics, the initial studies have been specialized to the following areas:

- a. Phonon interactions in solid-state materials.
- b. Generation in and radiation from solids.
- c. Acoustic-wave interactions, including both longitudinal and shear mode excitations.

As each of the investigations progress it is planned that specific experiments will be designed to check the theoretical results. Each of the above topics is discussed in detail in the following sections of this report.

2. Phonon Interaction in Solids (J. E. King)

2.1 Background. In considering phonon interactions in solids there are a number of possible effects which should be considered. One of the first that comes to mind is the interaction of a phonon wave with a current in a semiconductor. This gives rise to a traveling-wave phonon amplification where energy is converted from the electron beam to the phonon

wave. This particular phenomena is being investigated widely and is fairly well understood.

A second type of interaction to be considered is phonon-phonon interaction. The particularly interesting aspect here concerns parametric interactions which arise from a nonlinear ω - β diagram. The pump, signal, and idler waves must satisfy the standard criteria for parametric interaction, namely,

$$\omega_i = \omega_p - \omega_s$$

and

$$\beta_i = \beta_p - \beta_s , \quad (2.1)$$

where ω = radian frequency,

β = phase constant,

i = idler wave,

p = pump wave, and

s = signal wave.

If these conditions are satisfied it is possible to obtain gain of the signal wave. There are two possible conditions which will satisfy the above equations, one is the "forward" wave case where all waves (signal, idler and pump) travel with group velocities in the same direction, the second is a "backward" wave case where the signal wave has a group velocity in the opposite direction to those of the pump and idler waves. The characteristics of this interaction are beating-wave amplification for the "backward" wave and exponential gain for the "forward" wave.

Another type of interaction that should be considered is phonon paramagnetic resonance. This type of interaction is similar to electron paramagnetic resonance which utilizes electromagnetic waves. The characteristics of this type of interaction are an absorption of energy from the

phonon wave and a characteristic slowing of the wave due to dispersion. This suggests that since the group velocity is changed, the phase velocity ought also to change and this introduces a nonlinearity in the ω - β diagram for the phonon waves. In addition this mechanism gives rise to the phonon maser.

There are a number of other types of interaction which can occur, although most of them produce rather small effects. One, however, which should be considered is piezoelectric interaction which has been accounted for in the traveling-wave phonon amplifier since it is the mechanism by which the electron beam and phonon wave in the semiconductor are coupled. However it is possible that the electric and magnetic fields generated piezoelectrically might give rise to an interaction between the phonon wave and the lattice. In particular, there might possibly be an interaction between these fields and paramagnetic ions in the lattice.

From the brief discussion above it can be seen that it is possible to develop an amplifier which combines several of these interaction mechanisms. Two particular devices will be considered. The first is a parametric phonon amplifier using paramagnetic resonance to obtain the nonlinear ω - β diagram. The second is a phonon amplifier that relies on the electric and magnetic fields generated by a piezoelectric crystal interacting with a paramagnetic ion. The latter is very similar to the phonon maser except the method of interaction is slightly different. The primary effort this first quarter was on the first device.

2.2 Review of Theory. In order to understand the interaction mechanisms further, the fundamental theories will be reviewed below. To begin with consider the details of the parametric interaction theory.

The first account of this was published by P. K. Tien¹ in 1958. In this article power gain, bandwidth and noise are discussed for electromagnetic waves propagating along one-dimensional transmission lines. An extension of this idea to distributed reactance systems was carried out by Breitzer and Sard². Finally, Hsu³ calculated the gain and noise figure for parametric interaction. The basic assumption made in these analyses is that of a periodically varying dielectric constant along the direction of propagation. The wave equation is then solved for this variation in dielectric constant

$$\epsilon = \epsilon_0 [1 + \epsilon(z,t)] \quad . \quad (2.2)$$

The conditions of Eq. 2.1 which are typical for parametric interaction are obtained. In addition the power gain of the amplifier is calculated. For the "backward" mode the gain is

$$\text{Power gain} \propto \frac{1}{\cos^2(kz)} \quad . \quad (2.3)$$

For the "forward" mode we obtain

$$\text{Power gain} \propto \cosh^2(kz) \quad . \quad (2.4)$$

The same analysis can be extended to include phonon waves since all the basic quantities such as pressure, particle displacement and density, satisfy the wave equation providing that the interaction is small. This

-
1. Tien, P. K., "Parametric Amplification and Frequency Mixing in Propagating Circuits", Jour. of App. Phys., vol.29, pp. 1347-1357; September, 1958.
 2. Breitzer, D. I., Sard, E. W., "Low Frequency Prototype Backward-Wave Reactance Amplifier", Microwave Journal, vol. 2, pp. 34-37; August, 1959.
 3. Hsu, H., "Analysis of Backward Traveling-Wave Parametric Amplifiers", General Electric Company, TIS, No. R6OELS-3; 1960.

assumption depends on the perturbation of the density being small* which implies that the same analysis applies for one-dimensional phonon waves. The additional feature of phonon waves is that there is three-dimensional propagation and the propagation constants are in general anisotropic. In this analysis it is assumed that the density varies as a function of frequency and direction of propagation in the same way that the dielectric constant varies for reactance amplifiers. The above establishes the possibility of a traveling-wave parametric interaction providing a material can be found such that the parametric conditions of Eq. 2.1 are satisfied.

One possible way in which to introduce a nonlinearity in the ω - β diagram is to make use of acoustic paramagnetic absorption. Jacobsen and Stevens⁴ calculated the ω - β diagram for simple spin systems. A typical ω - β diagram is reproduced in Fig. 2.1 assuming no loss. Figure 2.2 shows the effect of loss on the ω - β diagram. The second figure is obtained as a generalization of the signal velocity changes observed by Shiren⁵. It is assumed that the group velocity and phase velocity form the usual Hilbert transform pair. Thus extrapolating the measurements made on the signal velocity, the curve for the phase velocity leads to an ω - β diagram of the type represented in Fig. 2.2. The size of the nonlinearity depends on the magnitude of the spin-phonon interaction.

The magnitude of the spin-phonon interaction is affected by the particular paramagnetic ion and also the type of crystal lattice.

*

See for example Morse, P. M., Vibration and Sound, McGraw-Hill, York, Pa., pp. 217-222; 1948.

4. Jacobsen, E. H., Stevens, K. W. H., "Interaction of Ultrasonic Waves with Electron Spins", Physical Review, vol. 129, pp. 2036-2044; March, 1963.
5. Shiren, N. S., "Measurement of Signal Velocity in a Region of Resonant Absorption by Ultrasonic Paramagnetic Resonance", Physical Review, vol. 128, pp. 2103-2112; December 1, 1962.

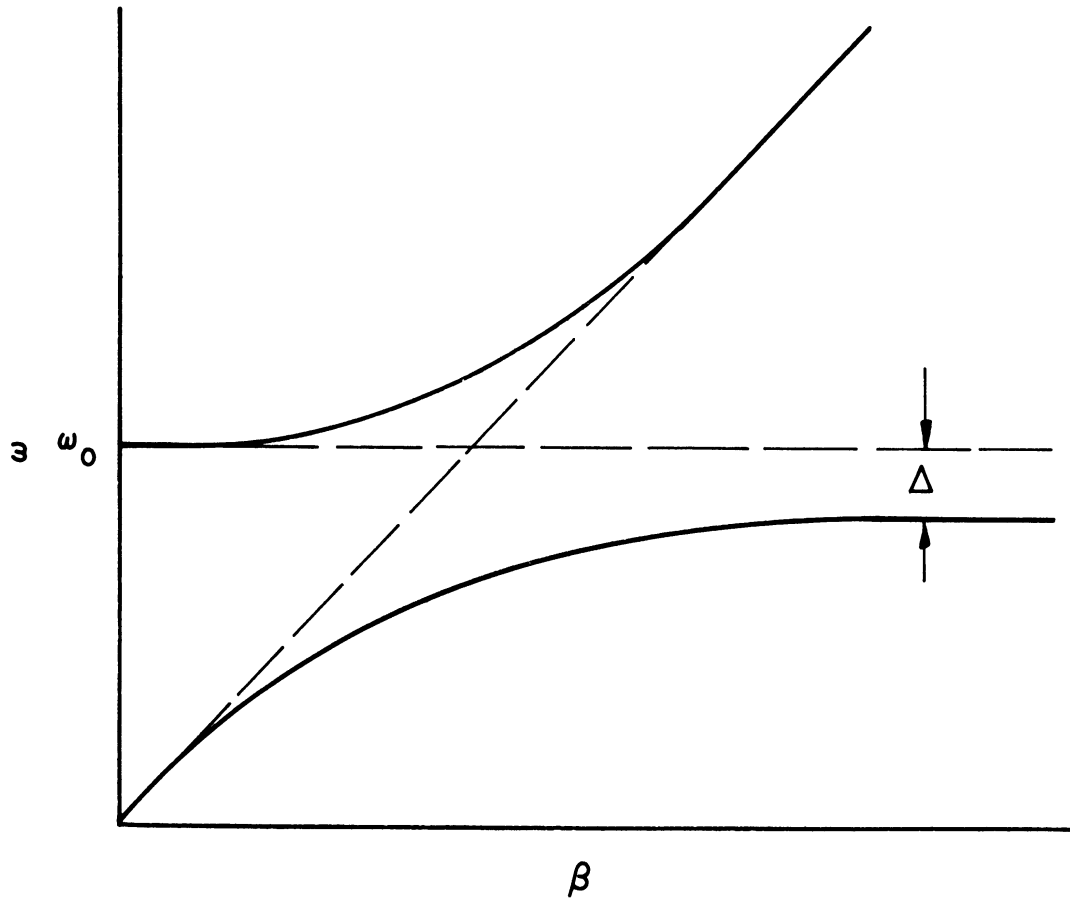


FIG. 2.1 DISPERSION RELATION BETWEEN ELASTIC WAVE FREQUENCY ω AND PHASE CONSTANT β . Δ IS STOP BAND NEAR SPIN RESONANCE FREQUENCY ω .

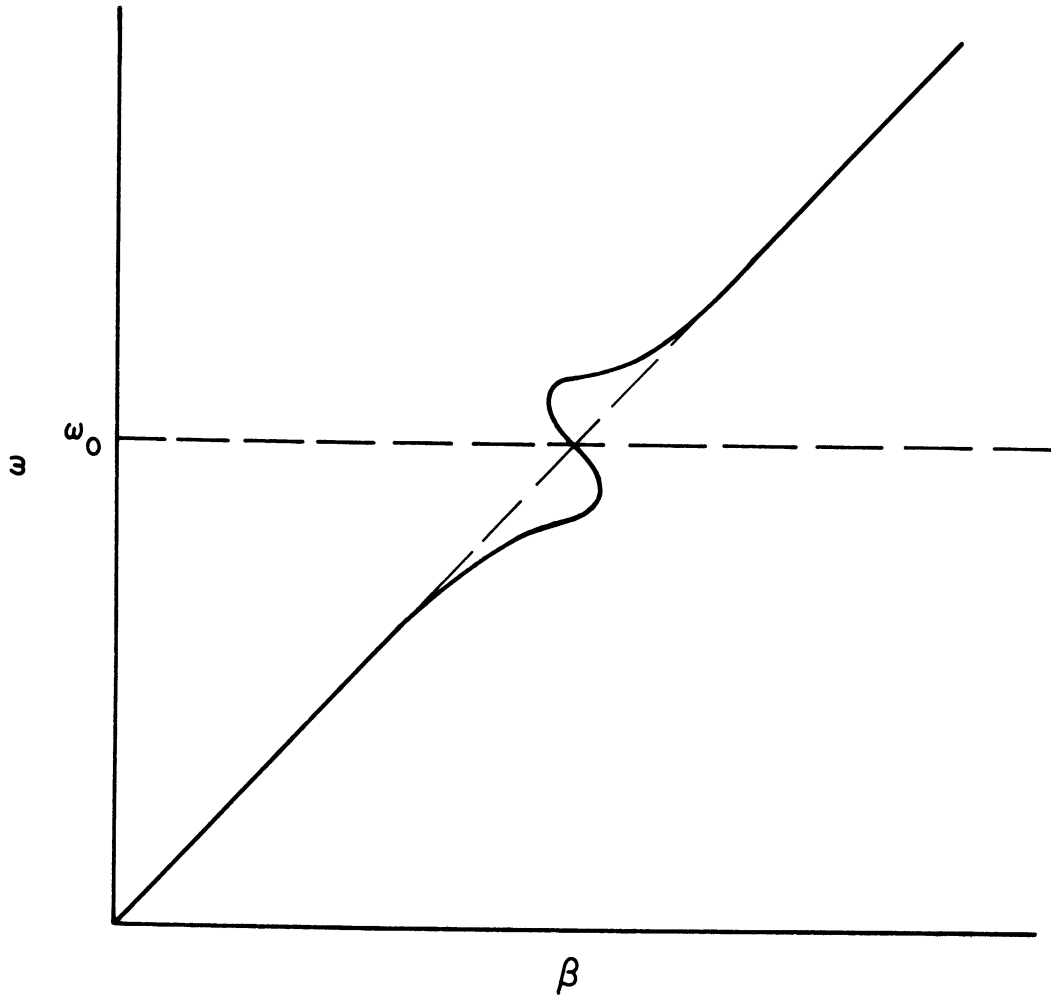


FIG. 2.2 DISPERSION RELATION BETWEEN ELASTIC WAVE FREQUENCY ω AND PHASE CONSTANT β WITH LOSS IN THE PARAMAGNETIC ABSORPTION NEAR SPIN RESONANCE FREQUENCY ω .

Investigations on spin-phonon interaction began in the early 1950's. However at that time the experimental investigations were limited to nuclear magnetic resonance because of the low frequency sound waves⁶. Since the advent of microwave ultrasonics in 1959, more investigations have been undertaken and most of these have been concerned with electron paramagnetic resonance. These investigations have been initiated in order to understand more about the spin-lattice relaxation time with regard to microwave electron paramagnetic resonance.

The theory of spin-phonon interaction was first worked out by Al'tshuler^{7,8}. This paper deals primarily with low frequency (megacycle) phonon waves. Since 1959 a number of papers have been written concerning the theory of spin-phonon interaction and the two most notable being one by Mattuck and Strandberg⁹ and the other by Al'tshuler, Kochelaev, and Seushin¹⁰. These consider the recent advances in microwave ultrasonics. Mattuck and Strandberg develop the spin-phonon Hamiltonian. From this Hamiltonian the absorption coefficient can be worked out. Al'tshuler et. al. have worked out the absorption coefficient for various paramagnetic ions in crystals¹¹.

-
6. Shutilov, V. A., "Stimulation of Ultrasonic Nuclear Magnetic Resonance, Review", Soviet Physics-Acoustics, vol. 8, pp. 303-319; April-June, 1963.
 7. Al'tshuler, S. A., "Resonance Absorption of Ultrasound in Paramagnetic Salts", Soviet Physics-JETP, vol. 1, pp. 29-36; July, 1955.
 8. Al'tshuler, S. A., "On the Theory of Electronic and Nuclear Paramagnetic Resonance Under the Action of Ultrasound", Sov. Phys.-JETP, vol. 1, pp. 37-44; July, 1955.
 9. Mattuck, R. D., Strandberg, M. W. P., "Spin-Phonon Interaction in Paramagnetic Crystals", Physical Review, vol. 119, pp. 1204-1217; Aug. 15, 1960.
 10. Al'tshuler, S. A., Kochelaev, B. I., Leushin, A. M., "Paramagnetic Absorption of Sound", Soviet Physics-Uspeski, vol. 4, pp. 880-903; May-June, 1962.
 11. Al'tshuler, S. A., Bashkirov, Sh. Sh., Leushin, A. M., "Theory of the Acoustic Paramagnetic Resonance in Crystals Containing Ions of the Iron Group", Soviet Physics-Solid State, vol. 3, pp. 1088-1090; Nov. 1961.

It is possible to work out the ω - β diagram using their theory from the Hamiltonian as Jacobsen and Stevens⁴ did. It is also possible to select crystals with various paramagnetic ions according to the magnitude of the spin-phonon absorption coefficient. In addition it is possible to determine the transition probabilities for spin-phonon interaction¹².

The second device, a piezoelectric phonon amplifier, utilizes still another phenomena. The type of interaction that is expected is similar to the phonon maser¹³. In addition to the possible phonon-spin interaction which is second order, the electric and magnetic fields traveling with a phonon wave can interact with the paramagnetic ions to produce regular maser action. The net result is a coupling back to the phonon wave to increase its magnitude through the piezoelectric coefficients. Considerable theoretical work is necessary on this project to understand more completely the nature of the interaction and its magnitude. It is hoped that this type of interaction would yield an effect of the same order of magnitude as the phonon-spin interaction.

2.3 Theory

2.3.1 Parametric Conditions. Let us consider a crystal lattice fixed in a coordinate system x,y,z in which we have traveling waves of frequency ω_p , ω_i , and ω_s for the pump, idler, and signal frequencies respectively. Now consider a second coordinate system x', y', z' moving with a velocity \vec{v} with respect to the x,y,z coordinates.

Recall from the Lorentz transformations of a plane wave, the frequencies convert as

-
12. Tucker, E. B., "Attenuation of Longitudinal Ultrasonic Vibrations by Spin-Phonon Coupling in Ruby", Physical Review Letters, vol 6, pp. 183-185; February 15, 1961.
 13. Tucker, E. B., "Amplification of 9.3 kmc/sec Ultrasonic Pulses by Maser Action in Ruby", Physical Review Letters, vol. 6, pp. 547-548; May 15, 1961.

$$\frac{\omega'}{\omega} = \frac{1 - v/c \cos \theta}{\sqrt{1 - (v/c)^2}} \quad (2.5)$$

Now considering the case where $v \ll c$

$$\omega' = \omega - \frac{v\omega}{c} \cos \theta \quad (2.6)$$

Recall that $\beta = v/c$, the phase constant and $\cos \theta = \vec{a} \cdot \vec{b}$,

thus

$$\omega' = \omega - \vec{v} \cdot \vec{\beta} \quad (2.7)$$

One now has the relations for the Doppler frequency in the moving coordinate system. They are

$$\omega'_p = \omega_p - \vec{v} \cdot \vec{\beta}_p \quad ,$$

$$\omega'_i = \omega_i + \vec{v} \cdot \vec{\beta}_i \quad ,$$

and

$$\omega'_s = \omega_s - \vec{v} \cdot \vec{\beta}_s \quad (2.8)$$

Parametric interaction becomes possible when the pump frequency is equal to the signal plus idling frequencies in any moving coordinate system. Thus

$$\omega_p = \omega_s + \omega_i \quad (2.9)$$

and

$$\omega'_p = \omega'_s + \omega'_i \quad (2.10)$$

Substituting the relations for the moving coordinate system into Eq.

2.6 gives

$$\vec{v} \cdot \vec{\beta}_p = \vec{v} \cdot \vec{\beta}_i + \vec{v} \cdot \vec{\beta}_s \quad (2.11)$$

If all waves have the same velocity then for the forward wave

$$\vec{\beta}_p = \vec{\beta}_i + \vec{\beta}_s . \quad (2.12a)$$

If the signal wave has an oppositely directed group velocity then for the backward wave

$$\vec{\beta}_p = \vec{\beta}_i - \vec{\beta}_s . \quad (2.12b)$$

Thus Eqs. 2.9 and 2.12 are the conditions to be satisfied for traveling-wave parametric interaction. If Eqs. 2.9 and 2.12 are multiplied by n (Planck's constant/ 2π) the following is obtained:

$$\hbar \omega_p = n \omega_s + n \omega_i , \quad (2.13)$$

$$\hbar \beta_p = n \beta_i + n \beta_s \quad (2.14a)$$

or

$$\hbar \beta_p = n \beta_i = n \beta_s . \quad (2.14b)$$

These equations represent the conservation of energy (Eq. 2.13) and momentum (Eq. 2.14).

2.3.2 Interaction of Traveling Waves. The following development applies to either phonon waves or to electromagnetic waves. For phonon waves, one has the wave equation

$$\nabla^2 \xi - k \frac{\partial^2}{\partial t^2} (\rho \xi) = 0 , \quad (2.15)$$

where ξ = displacement,

ρ = mass density,

$k = 1/P_0 \gamma_c$,

P_0 = equilibrium pressure and $\gamma_c = C_p/C_v$ the ratio of specific heats.

ρ is allowed to be time dependent since ρ is to vary with the pump wave.

For electromagnetic waves we have

$$\nabla^2 E - \mu_0 \frac{\partial^2}{\partial t^2} (\epsilon E) = 0 , \quad (2.16)$$

where E = electric field,

μ_0 = permeability, and

ϵ = dielectric constant.

In the above two wave equations a homogeneous and continuous media has been assumed. The density and dielectric constant are assumed to be time dependent, being perturbed by the pump wave. It is further assumed that the signal, pump, and idler waves are all plane waves. For phonon waves it is assumed that the attenuation constant is zero and that the lattice is perfect with no dislocations or imperfections. It is also assumed that the lattice is at a low temperature so that the number of thermal phonons is negligible at the frequencies of interest. In the case of the electromagnetic waves the space charge and conductivity of the medium are considered to be negligible. Thus one sees that the two wave equations are basically the same and a solution to either one is a representative solution of both. Note though that the assumptions are much more restrictive for the phonon wave than for the electromagnetic wave. This is mainly because isotropic perfect crystals with zero attenuation constant are hard to find. As a result of the similarity of the two equations, only a solution for the electromagnetic wave equation will be developed.

The dielectric constant will be assumed to be perturbed by the traveling wave at the pump frequency. Thus the dielectric constant can be written as

$$\epsilon = \epsilon_0 [1 + \zeta \cos (\omega_p t - \vec{\beta}_p \cdot \vec{\gamma})] , \quad (2.17)$$

with the pump wave traveling with a phase constant $\vec{\beta}_p$ in the direction $\vec{\gamma}$, the general coordinate vector given by

$$\vec{\gamma} = x \hat{i} + y \hat{j} + z \hat{k} .$$

Thus if the pump wave was propagating in the z-direction

$$\vec{\beta}_p \cdot \vec{\gamma} = \beta_{p_z} z .$$

A solution to the wave equation is assumed whose coefficients are functions of z but not of t. Then

$$\begin{aligned} E = & A_1(z) e^{j(\omega_1 t - \beta_1 z)} + A_2(z) e^{j(\omega_2 t - \beta_2 z)} \\ & + B_1(z) e^{-j(\omega_1 t - \beta_1 z)} + B_2(z) e^{-j(\omega_2 t - \beta_2 z)} . \end{aligned} \quad (2.18)$$

ω_1 and ω_2 represent the signal and idling frequencies.

The wave equation is given by Eq. 2.16 and the dielectric constant can be expanded as

$$\epsilon = \epsilon_0 \left\{ 1 + \frac{\zeta}{2} \left[e^{j(\omega t - \beta z)} + e^{-j(\omega t - \beta z)} \right] \right\} , \quad (2.19)$$

where

$$\omega = \omega_1 - \omega_2$$

$$\beta = \beta_1 - \beta_2 . \quad (2.20)$$

Substituting the assumed solution and the expression for the dielectric constant into the wave Eq. 2.16 and noting that $\beta^2 = \omega^2 \mu_0 \epsilon$, the following equation results

$$\begin{aligned}
 & e^{j(\omega_1 t - \beta_1 z)} \left[\frac{\partial^2 A_1}{\partial z^2} - j2\beta_1 \frac{\partial A_1}{\partial z} + \frac{\zeta}{2} A_2 \beta_1^2 \right] \\
 & + e^{j(\omega_2 t - \beta_2 z)} \left[\frac{\partial^2 A_2}{\partial z^2} - j2\beta_2 \frac{\partial A_2}{\partial z} + \frac{\zeta}{2} A_1 \beta_2^2 \right] \\
 & + e^{-j(\omega_1 t - \beta_1 z)} \left[\frac{\partial^2 B_1}{\partial z^2} + j2\beta_1 \frac{\partial B_1}{\partial z} + \frac{\zeta}{2} B_2 \beta_1^2 \right] \\
 & + e^{-j(\omega_2 t - \beta_2 z)} \left[\frac{\partial^2 B_2}{\partial z^2} + j2\beta_2 \frac{\partial B_2}{\partial z} + \frac{\zeta}{2} B_1 \beta_2^2 \right] = 0 . \quad (2.21)
 \end{aligned}$$

Note that A_1 and A_2 are coupled by ζ as are B_1 and B_2 . For the equation to be satisfied independent of time and distance each term must be individually zero. If in addition the A's and B's are assumed to be slowly varying functions of z , then the second derivatives can be considered small with respect to the term $\beta \partial/\partial z$. As a result two sets of first-order equations arise.

$$\frac{\partial A_1}{\partial z} = -j \frac{\zeta}{4} \beta_1 A_2 ,$$

$$\frac{\partial A_2}{\partial z} = -j \frac{\zeta}{4} \beta_2 A_1 , \quad (2.22)$$

and

$$\frac{\partial B_1}{\partial z} = +j \frac{\zeta}{4} \beta_1 B_2 ,$$

$$\frac{\partial B_2}{\partial z} = +j \frac{\zeta}{4} \beta_2 B_1 . \quad (2.23)$$

The solution of Eq. 2.22 for $\beta_1, \beta_2 > 0$ is

$$\begin{aligned} A_1 &= a_1 e^{j\alpha z} + b_1 e^{-j\alpha z} , \\ A_2 &= -\sqrt{\beta_2/\beta_1} [a_1 e^{j\alpha z} - b_1 e^{-j\alpha z}] , \end{aligned} \quad (2.24)$$

where $\alpha = \sqrt{\zeta^2 \beta_1 \beta_2}/16 = \sqrt{\beta_1 \beta_2}/4$. The solution of Eq. 2.23 is

$$\begin{aligned} B_1 &= a_2 e^{j\alpha z} + b_2 e^{-j\alpha z} , \\ B_2 &= \sqrt{\beta_2/\beta_1} [a_2 e^{j\alpha z} - b_2 e^{-j\alpha z}] . \end{aligned} \quad (2.25)$$

Recall A_2 and B_2 are the coefficients for the wave at frequency ω_2 and A_1 and B_1 are the coefficients for the wave at frequency ω_1 . The boundary conditions imposed are that a signal and a pump wave are applied at the input. Thus it is assumed that the signal is in phase at the input. The idler will be assumed to have a zero initial amplitude. Consequently the coefficients are such that

$$a_1 = b_1$$

and

$$a_2 = b_2 ,$$

in order to assure that the idler has zero amplitude at the origin. If the signal has amplitude E_0 at the origin then

$$a_1 = b_1 = a_2 = b_2 = \frac{E_0}{4} . \quad (2.26)$$

Combining this result with Eqs. 2.24 and 2.25 and substituting into Eq. 2.18, the assumed solution for E becomes

$$E = E_0 \cos \alpha z \cos (\omega_1 t - \beta_1 z) + E_0 \sqrt{\beta_2 / \beta_1} \sin \alpha z \sin (\omega_2 t - \beta_2 z) . \quad (2.27)$$

Substituting $\alpha = \zeta \sqrt{\beta_1 \beta_2} / 4$ yields

$$E = E_0 \cos \zeta z \sqrt{\beta_1 \beta_2} / 4 \cos (\omega_1 t - \beta_1 z) + E_0 \sqrt{\beta_2 / \beta_1} \sin \zeta z \sqrt{\beta_1 \beta_2} / 4 \sin (\omega_2 t - \beta_2 z) . \quad (2.28)$$

Now recall that $\omega = \omega_1 - \omega_2$ and $\beta = \beta_1 - \beta_2$.

If we let

$$\left. \begin{aligned} \omega_p &= \omega \\ \beta_p &= \beta \\ \omega_1 &= \omega_s \\ \beta_1 &= \beta_s \end{aligned} \right\} \text{and} \left. \begin{aligned} \omega_2 &= -\omega_i \\ \beta_2 &= -\beta_i \end{aligned} \right\} \quad (2.29)$$

for the forward wave, then

$$\begin{aligned} \omega_p &= \omega_s + \omega_i , \\ \beta_p &= \beta_s + \beta_i . \end{aligned} \quad (2.30)$$

Making these substitutions in Eq. 2.28 and using the fact that $\cos j \theta = \cosh \theta$ and $\sin j \theta = j \sinh \theta$, gives

$$\begin{aligned}
 E = & E_0 \cosh \left(\frac{\zeta z}{4} \sqrt{\beta_s (\beta_p - \beta_s)} \right) \cos (\omega_s t - \beta_s z) \\
 & + E_0 \sqrt{(\beta_p - \beta_s)/\beta_s} \sinh \left(\frac{\zeta z}{4} \sqrt{\beta_s (\beta_p - \beta_s)} \right) \sin (\omega_i t - \beta_i z) .
 \end{aligned}
 \tag{2.31}$$

This is the expression for field as a function of z and t for the signal and idler waves where both are in the forward direction. For backward waves $\beta_s < 0$ and $\beta_1 = -|\beta_s|$ is substituted in Eq. 2.29. Then

$$\begin{aligned}
 \omega_p &= \omega_s + \omega_i , \\
 \beta_p &= -|\beta_s| + \beta_i .
 \end{aligned}
 \tag{2.32}$$

Substituting in Eq. 2.28 for the backward wave field gives

$$\begin{aligned}
 E = & E_0 \cos \frac{\zeta z}{4} \sqrt{|\beta_s| (\beta_p + |\beta_s|)} \cos (\omega_s t + |\beta_s| z) \\
 & - E_0 \sqrt{(\beta_p + |\beta_s|)/|\beta_s|} \sin \frac{\zeta z}{4} \sqrt{|\beta_s| (\beta_p + |\beta_s|)} \sin (\omega_i t - \beta_i z) .
 \end{aligned}
 \tag{2.33}$$

This represents the electric field as a function of z and t for the signal and idler waves, the first term for the signal and the second for the idler. Note that the major difference between Eq. 2.31 and 2.33 is the dependence on ζ . In Eq. 2.31 for the forward wave there is exponential dependence and in Eq. 2.33 for the backward wave there is a beating-wave effect wherein energy is transferred between the idler and signal waves as a function of distance.

The power associated with the signal wave is proportional to the time average field squared.

For the forward signal wave the time average output E_0 field at position z is given by

$$E_s = \frac{E_o}{2} \cosh \frac{\zeta z}{4} \sqrt{\beta_s (\beta_p - \beta_s)} .$$

The input signal wave is just $E_o/2$ so that the power gain is proportional to

$$P_s \propto \cosh^2 \frac{\zeta z}{4} \sqrt{\beta_s (\beta_p - \beta_s)} . \quad (2.34)$$

For the backward wave, consider that the signal input is at $z = z_o$. Then the input signal is given by

$$E_s = \frac{E_o}{2} \cos \frac{\zeta z_o}{4} \sqrt{|\beta_s| (\beta_p + |\beta_s|)} .$$

The output is at $z = 0$ and is just $E_o/2$ so that the power output is proportional to

$$P_s \propto \frac{1}{\cos^2 \frac{\zeta z_o}{4} \sqrt{|\beta_s| (\beta_p + |\beta_s|)}} . \quad (2.35)$$

Therefore if the modulation parameter ζ is adjusted so that the argument of the cosine is nearly $\pi/2$, the denominator will be quite small giving a sizable gain.

2.3.3 Phonon Paramagnetic Resonance. The method of obtaining information about the spin-phonon interaction is to start with the total Hamiltonian for the crystal. This Hamiltonian includes terms which account for spin-spin interaction, lattice energy, free ion energy, and orbital coupling. The Hamiltonian can then be written as

$$|-\rangle = |-\rangle_L + |-\rangle_o + V + 2\beta \vec{S} \cdot \vec{H} + \lambda \vec{L} \cdot \vec{S} + \beta \vec{L} \cdot \vec{H} , \quad (2.36)$$

where β is the Bohr magneton,

λ is the spin-orbit coupling parameter,

\vec{S} and \vec{L} are the spin and orbital angular moments of the paramagnetic ion,

\vec{H} is the external d-c magnetic field,

V is the energy of the ion due to the crystalline electric field,

$|-\rangle_0$ is the energy of the free ion, and

$|-\rangle_L$ represents the lattice energy.

Under the assumption of harmonic forces between atoms in the crystal, the lattice Hamiltonian becomes

$$|-\rangle_L = \sum_{\rho} \hbar \omega_{\rho} \left(a_{\rho}^{\dagger} a_{\rho} + \frac{1}{2} \right) , \quad (2.37)$$

where a_{ρ}^{\dagger} and a_{ρ} are the phonon creation and annihilation operators.

They have the properties that

$$\begin{aligned} a_{\rho}^{\dagger} | \dots \eta_{\rho} \dots \rangle &= (\eta_{\rho} + 1)^{1/2} | \dots \eta_{\rho} + 1 \dots \rangle \\ a_{\rho} | \dots \eta_{\rho} \dots \rangle &= \eta_{\rho}^{1/2} | \dots \eta_{\rho} - 1 \dots \rangle , \end{aligned} \quad (2.38)$$

where η_{ρ} is the ρ th eigenvalue.

After a number of complicated perturbation calculations a spin-phonon interaction Hamiltonian can be calculated for direct interaction between phonons and spin. The following equivalent Hamiltonian involving spin and phonon operators results¹⁴:

$$\begin{aligned} |-\rangle_{sp} = \sum_{\substack{\rho, f \\ i \geq j}} A^{f\rho} P_{\rho} [& \hbar \nu b_{i i}^f (\lambda S_i) - b_{i i}^f (\lambda^2 S_i S_i + \lambda \beta (S_i H_i + H_i S_i)) \\ & + b_{i j}^f \{ \lambda^2 (S_i S_j + S_j S_i) + \lambda \beta (S_i H_j + H_i S_j + S_j H_i + H_j S_i) \}] \end{aligned} \quad (2.39)$$

14. Mattuck, R. D., Strandberg, M. W. P., Loc. Cit. p. 1208.

where b_i^f and b_{ij}^f represent coupling parameters between orbital levels through the orbital angular momentum L and the perturbation of the crystalline electric field.

$A^{f\rho}$ represents the amplitudes associated with the normal modes of vibration of the lattice and P_ρ is the creation and annihilation operator $= a_\rho^+ + a_\rho$. This equation represents a multipole expansion of the interaction in terms of the spin operators. The terms linear in S_i are the dipolar terms, with those quadratic in S_i being quadrupolar.

Using this interaction Hamiltonian it is possible to calculate matrix elements which will yield the absorption coefficient of spin-phonon interaction between two spin states i and j . Before doing this the Hamiltonian can be simplified under certain cases. The first simplification distinguishes between when the total effective spin quantum number $S' = 1/2$ or when $S' > 1/2$.

Case I. $S' = 1/2$.

When $S' = 1/2$ we have what is termed a Kramer's Doublet. The two energy levels are then split uniformly by the Zeeman interaction. The terms linear in S_i are the dipolar expansion and should be the largest. The $S_i S_j$ terms stimulate transitions of 0 or ± 2 in quantum number, since the S_i operators operate 0 or ± 1 , and the term $(S_i S_z + S_z S_i)$ exactly cancels. The terms remaining are then linear in S_i since the $S_i S_i$ terms also give 0 or ± 2 transitions. Note with two levels a change of ± 2 is not allowed. The results is then

$$|-\rangle_{sp} = \sum_{\substack{\rho, f \\ i \geq j}} A^{f\rho} P_\rho [h\lambda b_i^f \lambda S_i - b_{ii}^f \lambda \beta (S_i H_i + H_i S_i) + b_{ij}^f \lambda_\rho (S_i H_j + H_i S_j + S_j H_i + H_j S_i)] \quad (2.40)$$

Take Eq. 2.36 and make the following substitutions:

1. $\vec{H} = H_z \hat{z}$,
2. $h\nu = E_k - E_{k'} = g_{kk'} \beta H$,
3. The phonon wave is an x-directed longitudinal wave, and
4. Define $\bar{n}_\epsilon = \sum_{f'} B_f \lambda \beta H_z (g_{kk'} b_x^f + b_{zx}^f)$.

It is then possible to reduce the interaction Hamiltonian to

$$|-\rangle_{sp} = \bar{n}_\epsilon (U_{n+1} - U_{n-1}) S_x^n , \quad (2.41)$$

where n represents the paramagnetic ion at location n in the lattice.

Equation 2.37 is exactly the same interaction Hamiltonian used by Jacobsen and Stevens¹⁵ in the derivation of the dispersion relation for $S' = 1/2$.

Case II. $S' > 1/2$.

For this case, some terms can be dropped on the basis of their small size. In general $\lambda \gg \beta H$ and $h\nu$ so that only terms proportional to λ^2 will contribute. This leaves

$$|-\rangle_{sp} = \sum_{\substack{\rho, f \\ i > j}} A^{f\rho} P_\rho [b_{ii}^f \lambda^2 S_i S_i + b_{ij}^f \lambda^2 (S_i S_j + S_j S_i)] . \quad (2.42)$$

Using this form it is possible to generate the terms that Al'tshuler, Kochelaev and Leushin¹⁶ use in calculating the absorption coefficients for various paramagnetic ions. The procedure is to calculate the matrix elements between various levels. In addition this form can be simplified

15. Loc. Cit.

16. Loc. Cit.

in particular cases to simple interaction Hamiltonians. For $S' = 1$ this can be simplified to the result used by Jacobsen and Stevens.

2.3.4 Theoretical Conclusions. Using the spin-phonon Hamiltonian, Al'tshuler, Kochelaev, and Levshin¹⁷ have calculated the coefficients of sound absorption. These are summarized in the tables below.

Table 2.1

Coefficients of Sound Absorption for Ions with

$$S' = 1/2. \sigma = A \frac{v^4}{T} \times 10^{-40} \text{ cm}^{-1}$$

Configuration and term of ion	Spin	Ion	A
d ¹ 2D	S' = S = 1/2	Ti ³⁺	10 ⁴
d ⁷ 4F	S' = 1/2 S = 3/2	Co ²⁺	10 ²
d ⁹ 2D	S' = S = 1/2	Cu ²⁺	1

where S = spin of free ion, S' is effective spin of lattice site.

17. Loc. Cit.

Table 2.2

Coefficients of Sound Absorption for Ions with

$$S' > 1/2. \quad \sigma = A \frac{\nu^2}{T} \times 10^{-19} \text{ cm}^{-1}$$

Configuration and term of ion	Spin	Ion	A
d ² 3F	1	V ³⁺	10 ⁶
d ³ 4F	3/2	Cr ³⁺ V ²⁺	1
d ⁴ 5D	2	Cr ²⁺ Mn ³⁺	10 ⁵
d ⁶ 5D	2	Fe ²⁺	10 ⁶
d ⁸ 3F	1	Ni ²⁺	10 ³

Table 2.3

Coefficients of Absorption of Longitudinal Sound Waves in Ethylsulfates of Rare-Earth Ions with an Even Number of

$$\text{Electrons. } \sigma = A \frac{\nu^2}{T} \times 10^{-13} \text{ cm}^{-1}$$

Ion	No. of Doublet	Interval Between Doublet and Ground State (in cm ⁻¹)		Ion	No. of Doublet	Interval Between Doublet and Ground State (in cm ⁻¹)	
		A	A			A	A
Pr ³⁺	1	0	1.7	Ho ³⁺	1	4	7.3
	2	170	8.8		2	47	15.8
	3	212	1.7		3	60	150.1
Eu ³⁺	1	270	800.7		4	139	0
T _b ³⁺	1	7	3.7		5	141	1.5
	2	24	10.9		6	197	150.1

Table 2.3 (Cont.)

Ion	No. of Doublet	Interval Between Doublet and Ground State (in cm^{-1})	A	Ion	No. of Doublet	Interval Between Doublet and Ground State (in cm^{-1})	A
	3	26	60.8	Tm^{3+}	1	14	5.6
	4	50	10.5		2	26	12.0
					3	98	49.4
					4	129	13.4

Table 2.4

Coefficients of Absorption of Sound. Rare-Earth Ions with Odd Number of Electrons. $\sigma = A \frac{\nu^4}{T} \times 10^{-40} \text{ cm}^{-1}$

Ion	A
Nd^{3+}	600
Ce^{3+}	10^6

Based on this calculated data, the absorption coefficients will be compared for various ions. Assume $\nu = 10^9 = 1 \text{ Gc}$, then

$$\sigma_{\text{Ti}^{3+}} = 1/T ,$$

$$\sigma_{\text{Cr}^{3+}} = 1/10T ,$$

$$\sigma_{\text{Fe}^{2+}} = 10^5/T ,$$

$$\sigma_{\text{Pr}^{3+}} = 1.7 \times 10^5/T , \text{ and}$$

$$\sigma_{\text{Ce}^{3+}} = 100/T .$$

Note in general that the rare-earth ions have the largest absorption coefficient. This is due to the fact that for rare-earth ions, the outer electrons shield the ion from changes in crystalline field so that it is more sensitive to orbital changes. Note also that Cr^{3+} corresponds to the configuration found in ruby and that it has the smallest absorption coefficient.

Based on this data it is possible to select a material for high absorption coefficient. It appears that semiconductors can provide a suitable host lattice for some of these ions and in particular the rare-earth ions. In addition there is the possibility that these levels will be unequally spaced because of lattice distortions. This means that it might be possible to use these crystals for a phonon maser.

The absorption coefficients all contain frequency to some power in the numerator and temperature in the denominator. Thus in order to increase the absorption coefficient the frequency must be increased and the temperature lowered. However by increasing the frequency the attenuation constant of the material increases¹⁸. Thus a compromise between increasing σ and α must be reached.

It is interesting to note that although ruby has the lowest absorption coefficient it has been the material most often used experimentally. The phonon maser was demonstrated using ruby. However, Shiren¹⁹ used Ni^{2+} and Fe^{2+} and noted that the absorption for Fe^{2+} was larger than that for Ni^{2+} as is predicted by Table 2.2. Shiren also noted about a 20 percent slowing of the signal velocity for Fe^{2+} and only about 5 percent for Ni^{2+} which would also be predicted by the absorption coefficients.

18. Tannenwald, P. E., "Microwave Ultrasonics", Microwave Journal, vol. VI, pp. 61-65; December, 1963.

19. Loc. Cit.

This amount of change in the signal velocity should result in a significant change in the phase velocity. These quantities are related by the normal dispersion relation so that a sizable change in the phase constant is expected. This will result in an ω - β diagram similar to that of Fig. 2.2.

Parametric interaction of phonon waves is a general property of all materials having a suitable ω - β diagram. From the above discussion semiconductor materials with rare-earth dopants would seem to be one of the more appropriate materials. However, because of the availability of optically finished ruby rods previously used for a small laser, experimental effort has been channeled toward measuring the ω - β diagram for phonon waves in these rods. Acoustic paramagnetic resonance will occur for any suitable paramagnetic materials so that information gained from this investigation will be useful in any experiment involving acoustic paramagnetic resonance.

2.4 Experimental Apparatus. In order to construct a possible phonon parametric amplifier, more detailed knowledge of the ω - β diagram is required. Since the wavelength of phonon waves approaches optical wavelengths, the material needs to be polished flat and parallel on the end surfaces. Several small ruby rods for a laser are available. Consequently attempts have been made to measure the ω - β diagram. The method of measurement is to resonate the length of the rod by a pulse several times as long as the transit time through the rod. The resonance causes the reflected wave to add in phase with the input pulse and cause a build-up of phonon waves in the material. Then by adjusting the magnetic field for paramagnetic resonances, the phase velocity will change, thus changing the apparent length of the rod. Consequently as the magnetic field is swept, the rod will change from resonance to antiresonance, etc.

By measuring the change in field between resonant points and knowing the change in phase between these resonances, it is possible to construct an ω - β diagram.

As mentioned earlier, the frequency should be increased to increase the absorption coefficient. It is hoped that these experiments can be done first at room temperature. However, the material attenuation constant increases extremely rapidly above 1000 mc. Consequently, attempts will be made to observe the ω - β diagram for phonon waves in the UHF region, 300 to 700 mc. Another reason for this is that it is difficult to find a long pulse ($> 50 \mu$ sec) source at much higher frequencies. The long pulse is needed because the two-way transit time of the ruby rod is 12μ sec.

In attempting to obtain acoustic echoes at these frequencies, a wideband transducer was obtained so that the frequency could be changed easily. The transducer, an x-cut quartz crystal, giving longitudinal waves has a fundamental resonance of 1.4 mc. The ruby rod has resonances every 70 kc because of its much greater length. The transducer is mounted at the end of an open-circuited transmission line which gives maximum electric field to couple piezoelectrically with the phonon wave in the quartz. This setup gives wideband response because of its lack of tuned circuits. The transducer is then bonded mechanically onto the quartz. Figure 2.3 is a drawing of the transmission-line transducer. Using this equipment, echoes have been seen for frequencies up to 200 mc. Because of equipment bandwidths, echoes have not been seen at any higher frequencies. Much of the effort in the last few months has been to extend the frequency to higher values. It is felt that when phonon echoes

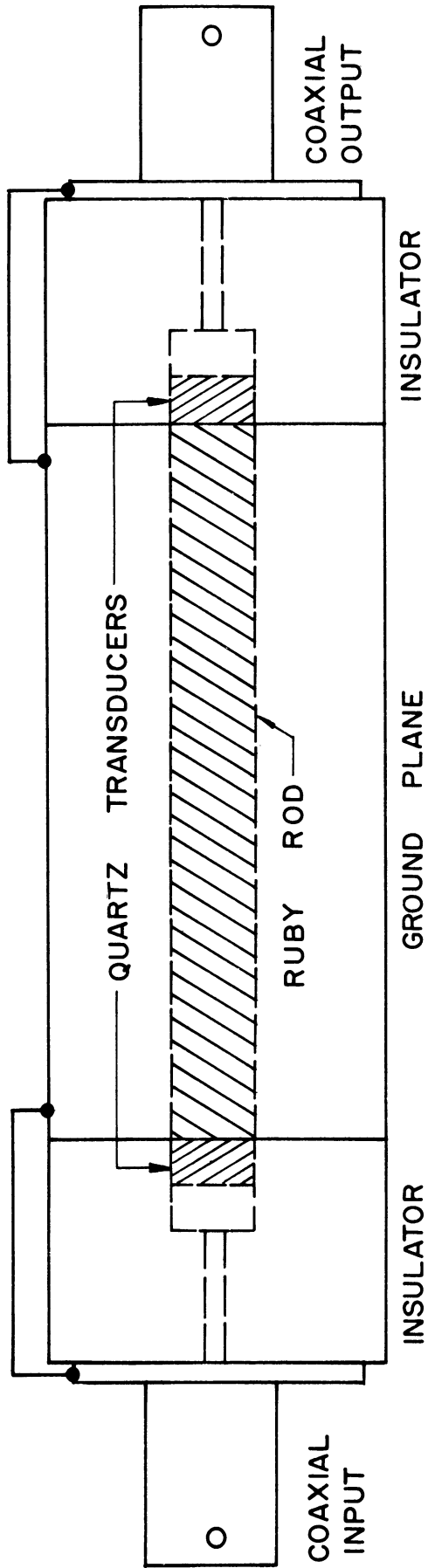


FIG. 2.3 TRANSMISSION LINE TRANSDUCER.

can be seen at 500 mc then it is worthwhile to attempt phonon paramagnetic resonance experiments. One method which might have to be used is to replace the wideband transducer with a cavity.

2.5 Program for the Next Quarter. Further work will be done on improving the coupling of phonon waves. This will be one of the major efforts for this next quarter. When the frequency is increased, the ω - β diagram will be investigated.

In addition the analysis leading to the absorption coefficients will be reviewed and a material will be selected for further studies.

If time permits, the theoretical analysis of the second type of device, piezoelectric phonon amplifier, will be investigated.

3. Radiation from Solids (D. C. Hanson)

3.1 Introduction. A number of reports,^{1,2,3} have appeared in the literature in the past few years concerning bulk oscillations in solids. This has had the effect of creating considerable interest in this phenomenon; however, for the most part, only experimental evidence of oscillation and radiation has been presented.

Previous to this, the junction characteristics of semiconductors have been utilized almost exclusively. This phenomenon has necessitated relatively little understanding of the basic transport and interaction mechanism in bulk homogeneous semiconductors since only the nonlinear junction capacitance or resistance was utilized. The former predominates

-
1. Larrabee, R. D., Steele, M. C., "The Oscillistor-New Type of Semiconductor Oscillator", Jour. of Appl. Phys., vol. 31, No. 9, pp. 1519-1523; September, 1960.
 2. Misawa, T., and Yamada, T., "Microwave Observation of Carrier Behavior in Oscillistors", Japanese Jour. of Appl. Phys., vol. 2, No. 1, p. 19; January, 1963.
 3. Gunn, J. B., "Microwave Oscillations of Current in III-V Semiconductors", Solid State Communications, vol. 1, pp. 88-91, Pergamon Press Inc.; 1963.

in varactor diodes used in parametric amplifiers to demonstrate effective input noise temperatures approaching that of the maser⁴.

The source of the reported bulk oscillation in semiconductors appears to be due to two distinctly different mechanisms:

a. The "oscillistor", a name coined by Larrabee and Steele¹ for electron-hole plasma oscillations in which helical instabilities occur in the bulk semiconductor in the presence of a magnetic field greater than a certain critical value. An ohmic contact is required on one surface of the bulk semiconductor and a p-n junction on another surface in order to inject minority carriers with a density approximately equal to the majority carrier density.

b. The "Gunn Radiation Experiment" in which only a high electric field is applied to a thin slab of homogeneous III-V compound semiconductor with two ohmic contacts and hence only majority carriers are involved. Significant amounts of microwave radiation, i.e., 0.5 watt at 1 Gc and 0.15 watt at 3 Gc, has been obtained at room temperature³.

In the following sections of this report these phenomena will be described in greater detail along with some conjecture as to the factors controlling the oscillation and/or radiation. A theory is proposed to explain the previously unexplained "Gunn Radiation Experiment".

3.2 Theory of Operation and Experimental Evidence

3.2.1 "Electron-Hole Plasma Oscillations" in a Magnetic Field (The "Oscillistor"). Larrabee and Steele¹ were the first to experimentally examine this type of bulk oscillation in detail. Their evidence included the following observations:

4. Hanson, D. C., Fink, H. J., Uenohara, M., "Varactor Diode Amplifier at Liquid Helium Temperature", Digest of 1963 Solid-State Circuits Conference, Philadelphia, Pa., pp. 54-55, Feb. 20-22, 1963.

1. Frequency: Few kc to 10 mc, depending mainly on the magnetic field, the orientation of the E and H fields and surface conditions. The frequency was independent of the external circuit.

2. Waveform: Usually periodic but not sinusoidal. Noise often appeared incoherently with high E and/or H fields.

3. Externally Applied Fields: An applied H field above a certain critical threshold (a function of applied E field) is required for oscillation. Also, a transverse component of H is required relative to E, otherwise only noise results.

4. Contacts and Surface: The bulk semiconductor volume was large enough that the contacts only served the function of injecting minority carriers and allowing current flow. Reflection effects at the contacts were negligible.

The surface appears to play a dominant role in this type of oscillation since oscillation only occurs when the transverse component of H was oriented so as to force the electrons to the surface rather than into the bulk semiconductor. Large magnetoresistance was observed whenever oscillation occurred due to enhanced surface recombination.

Glicksman⁵ has presented a relatively coherent analysis of a cylindrical electron-hole plasma oscillation in a magnetic field. By solving the steady-state case for injected minority carriers, with recombination only at the surface, and then assuming a helical density perturbation propagating along the cylindrical axis, Glicksman derives an oscillation threshold in the H vs. E plane as a function of b (the ratio of electron mobility to hole mobility). He finds that the lowest

5. Glicksman, M., "Instabilities in a Cylindrical Electron-Hole Plasma in Magnetic Field", Phys. Rev., vol. 124, No. 6, p. 1655, December 15, 1961.

frequency of oscillation is proportional to $1/a^2$ and the threshold E field is proportional to $1/a$, where a is the radius of the cylinder.

To take account of the surface, Glicksman simply assumes a minority carrier density ratio at the surface relative to that at the center of the cylinder. He has failed to consider the possibility of a large density of surface states⁶ and their effect on the Fermi level near the surface. Law⁷ and others have shown experimentally that such surface states effectively "clamp" the surface Fermi level relative to the surface potential barrier, an effect similar to surface "channeling" observed in transistors⁸. The conclusion is that a considerable part of the outward radial drift of holes and electrons, required for oscillation, could be contributed by the transverse gradient of the Fermi level with only an applied axial electric field.

Misawa and Yamada² have conducted an investigation of Glicksman's prediction of helical instabilities by observing the conductivity modulation on a 24 Gc carrier produced by electron-hole plasma oscillations. By moving a cylindrical germanium sample transversely in reduced height K-band waveguide with various magnetic field orientations, they found that helical density modulation does indeed exist. The frequency of oscillation was approximately 12.5 kc.

The utility of these electron-hole plasma oscillation phenomena appears to be more academic than potentially useful unless the effect were utilized to obtain amplification in the plasma frequency range from

-
6. Hannay, N. B., ED., "Semiconductors", (American Chemical Society Monograph No. 140), Reinhold Publishing Corp., New York, p. 685; 1959.
 7. Ibid, p. 705.
 8. Brown, W. L., "N-Type Surface Conductivity on p-Type Germanium", Phys. Rev., vol. 91, p. 518; August 1, 1953.

10 kc to 10 mc. It is apparent from the waveform of the plasma oscillation that many modes of oscillation usually exist. This type of electron-hole plasma oscillation could be quite useful, however, in the study of surface properties.

3.2.2 The "Gunn Radiation Experiment". J. B. Gunn of IBM has presented papers at two technical conferences (IEEE Solid State Device Research Conference, East Lansing, Michigan, June 14-16, 1963; and 1963 Electron Device Meeting, Washington, D. C., October 31-November 1, 1963) in addition to publications of results³ of the generation of significant amounts of microwave power directly from a pulsed d-c source applied to a thin slab of III-V semiconducting material. The interest in the phenomena is apparent from the above presentations but only experimental evidence has been presented. No theory has been presented to explain the radiation mechanism of this potentially significant device, however, such a theory must be developed before this phenomena can be utilized to the fullest extent for radiation and/or amplification.

The following sections of this report will review the experimental results, make a conjecture concerning the theory of operation and set forth a proposed experimental and theoretical analysis to evaluate this radiation phenomenon.

1. Experimental Results: Gunn's experiment was conducted at room temperature with zero magnetic field, and only an applied E field to n-type GaAs and n-type InP which had two ohmic contacts. The samples were approximately 0.020 inch on a side and the length between contacts, for which oscillation occurred, varied in the range from 0.0008 inch and 0.008 inch. The frequency of oscillation was inversely proportional to the specimen length and was in the range from 500 mc to 6000 mc. The critical value of electric field was between 2000-4000 volt/cm, producing a carrier

velocity of 10^7 cm/sec. The period of the observed oscillation was almost exactly the transit time between the contacts calculated from this velocity.

The peak microwave power delivered, with approximately one ohm resistors terminating the input and output, was 0.5W at 1Gc and 0.15W at 3Gc for a GaAs specimen.

Four possible mechanisms for the oscillation and radiation were suggested³ and subsequently rejected because the critical drift velocity is either several times too high or too low to justify the mechanism.

2. Conjecture Concerning the Radiation Mechanism: The difficulty in substantiating the radiation mechanism is readily apparent. However, due to Gunn's report³ that the oscillation condition is critically dependent on achieving a drift velocity of approximately 10^7 cm sec⁻¹ and hence a certain critical value in the number of injected electrons with only an E field applied and that only noise results for specimens longer than about 0.008 inch between the ohmic contacts, one is led to believe that the radiation is caused by stimulated emission of Bremsstrahlung from electrons decelerated in passing nuclei⁹. This conjecture is further substantiated by the statement³ that radiation is strongest in GaAs. Published data¹⁰ indicate that specimens of GaAs, which have been grown to this date, have net impurity concentrations greater than 10^{16} cm⁻³. These added impurity centers increase the probability of stimulated emission of Bremsstrahlung in bulk semiconductors as will be pointed out in the following section.

-
9. Panofski, W. K. H., Phillips, M., Classical Electricity and Magnetism, Reading, Massachusetts, Addison-Wesley Publishing Co., Inc., p. 361; 1962.
 10. Willardson, R. K., Goerring, H. L., Eds., Compound Semiconductors, vol. 1, Reinhold Publishing Corporation, New York, p. 388; 1962.

Marcuse^{11,12} has presented a very worthwhile analysis of stimulated emission of Bremsstrahlung. By utilizing certain of the quantum mechanical expressions of Heitler¹³ for the scattering of a stream of electrons in a Coulomb field, Marcuse¹¹ develops expressions for the differential scattering cross section for emission and absorption of plane electron waves incident on the Coulomb field of a nucleus. By utilizing conservation of energy and momentum, along with certain simplifying assumptions, he shows that stimulated emission should exist if the direction of electron velocity is within an angle of 54 degrees of the electric field vector stimulating the radiation and that absorption exists for larger angles. This could be the explanation for Gunn's report that only noise results for samples longer than a certain length, since with longer samples the individual electron velocity vectors would tend to diverge

By defining the loaded Q of the cavity in which the radiation occurs by¹⁴

$$Q_L = \frac{\omega NV}{n'} \quad , \quad (3.1)$$

where ω = angular frequency,

N = photon density,

V = volume of cavity, and

n' = number of photons dissipated per second to satisfy the condition for oscillation,

-
11. Marcuse, D., "Stimulated Emission of Bremsstrahlung", B.S.T.J., vol. XLI, No. 5, pp. 1557-1571, September, 1962.
 12. Marcuse, D., "A Further Discussion of Stimulated Emission of Bremsstrahlung", B.S.T.J., vol. XLII, No. 2, pp. 415-430; March, 1963.
 13. Heitler, W., The Quantum Theory of Radiation, Third Edition, Oxford; 1954.
 14. Marcuse, D., "Stimulated Emission of Bremsstrahlung", B.S.T.J., vol. XLI, No. 5, p. 1566, September, 1962.

Marcuse derives the following equation for the onset of oscillation¹⁴ with electron velocities parallel to the E vector stimulating the emission

$$N_e \left(\frac{N_n}{V} \right) = \frac{\pi \epsilon_0^3 m_e^3 v^4 f^3}{4 e^6 Z^2 Q_L \left[\left(\ln \frac{2 m_e v^2}{hf} \right) - 1 \right]}, \quad (3.2)$$

where N_e = number of electrons penetrating a unit area per unit time,
 N_n = ion concentration,
 V = volume of specimen,
 v = electron velocity,
 f = frequency of oscillation,
 e = electronic charge,
 m_e = electronic effective mass,
 Z = atomic number of nucleus,
 h = Plank's constant, and
 ϵ_0 = dielectric constant of material.

Equation 3.2 can be applied to determine the condition for oscillation in a thin slab of bulk GaAs with velocity (v), volume (V), and frequency (f) reported by Gunn³.

The following parameter values will be used:

$$\begin{aligned} v &= 10^7 \text{ cm sec}^{-1}, \\ f &= 3 \times 10^9 \text{ cps}, \\ Z &= 22 \text{ (average for Ga and As)}, \\ Q_L &= 10^3, \\ m_e &= 0.034 m_0^{15}, \text{ (n-type GaAs)}, \\ V &= (4 \times 10^{-2} \text{ cm}) \times \pi (10^{-1} \text{ cm})^2/4 = 3.14 \times 10^{-4} \text{ cm}^3, \\ \epsilon_0 &= 12.5, \text{ dielectric constant of GaAs}^{16}. \end{aligned}$$

15. Bude, R. H., Photoconductivity in Solids, J. Wiley and Sons, Inc., New York, p. 209; 1960.
16. Hilsum, C., Rose-Innes, A. C., Semiconducting III-V Compounds, Pergamon Press, New York, p. 181; 1961.

Then for the start of oscillation at 3Gc one must have

$$N_e \left(\frac{N_n}{V} \right) \Big| = \frac{4.24 \times 10^{23}}{\text{cm}^3} \times \left(\frac{1}{\text{cm}^2 \text{ sec}} \right) . \quad (3.3)$$

If a current density of 10 amperes/cm² is applied, the required ion density for oscillation is

$$\left(\frac{N_n}{V} \right) = 6.8 \times 10^3 \frac{\text{nuclei}}{\text{cm}^3} . \quad (3.4)$$

This low impurity density requirement for oscillation at 3Gc will be discussed in the following section concerned with radiated power to further justify the speculation that stimulated emission of Bremsstrahlung explains the Gunn radiation experiment.

Marcuse calculates in his second paper¹² the available power from this mechanism using fourth-order perturbation theory. He assumes a model for the nucleus which allows electron shielding by assuming a scattering potential $V = -Ze^2\epsilon^{-\gamma r}/r$, where γ is the exponential shielding constant. He obtains the important result that the available radiated power should go as the fifth power of frequency. His expression for the radiated power¹⁷ (with one correction) is

$$P_r = \frac{2 \pi^2 h^2 f^5 V}{e^2 v^2} \left(\frac{1}{Q_L} - \frac{1}{Q_i} \right) \left[1 - \frac{\pi m^3 v^4 f^3 V}{4 e^6 Z^2 Q_L N_n N_e \ln \left(\frac{2}{\sqrt{\epsilon^2 + \eta^2}} \right)} \right] , \quad (3.5)$$

where all quantities are as previously noted and in addition

$$Q_i = \text{unloaded } Q \text{ of the cavity, } Q_i \gg Q_L,$$

$$\epsilon = hf/mv^2, \text{ and}$$

$$\eta = e^2 Z^{1/3} / hv.$$

17. Marcuse, D., "A Further Discussion of Stimulated Emission of Bremsstrahlung", B.S.T J., vol. XLII, No. 2, p. 426; March, 1963.

Using this relationship and the parameter values previously used for the small GaAs specimen gives between 0.1 watt and 1.0 watt of power available at 1000 Gc. Marcuse points out that the limiting factor in achieving such power at frequencies above 100 Gc is the high required product of $N_e N_n$ for oscillation. However, this limitation does not appear to hold for a semiconductor such as GaAs with large impurity and lattice nuclei concentrations, where large electron current concentrations can be tolerated and where $v \ll c$.

It is appropriate to speculate on the mechanism for generating on the order of 0.5 watt of power at 1Gc, as Gunn has reported³ since the strong f^5 power relationship indicates that less than 10^{-10} watts would be available at this frequency.

From the length of Gunn's GaAs specimen for radiation at 3Gc, i.e., ≈ 0.004 cm, one can determine that this length is approximately a half wavelength at 1000 Gc, with $\epsilon_0 = 12.5$. Thus if a mode at 1000 Gc mixes with other crystal modes as it certainly will with nonlinearities from this much power, it is possible to generate difference frequencies in the microwave frequency range with considerable available power. The required ion density for oscillation at 1000 Gc is calculated from Eq. 3.2 as

$$\left(\frac{N_n}{V} \right) = 1.2 \times 10^{12} \frac{\text{nuclei}}{\text{cm}^3} . \quad (3.6)$$

Thus it is seen that the restriction stated by Marcuse, of having insufficient electron and ion densities at the higher frequencies where significant amounts of power are available, should not limit GaAs with a moderate current density of 10 amperes/cm² since the stated impurity concentration¹⁰ is probably at least 10^{16} nuclei per cm³. It appears that some of the parameter values can be relaxed and still achieve

oscillation at 1000 Gc since we have a factor of 10^4 cm^{-3} available from impurity density and the additional scattering from lattice sites is not included.

3.3 Proposed Experiment. In order to substantiate that this mechanism is responsible for the observed radiation an experiment will be conducted to determine the power spectrum of the radiation in the submillimeter and low infrared spectrum in addition to tuning the circuit in the region below 10 Gc for the observed radiation. This will involve a circuit such as shown schematically in Fig. 3.1. The circuit will be tuned coaxially for the observed radiation below 6 Gc and in addition the bulk semiconductor will be at one focus of a confocal ellipse or Fabry-Perot resonator. At the other focus will be a detector of radiation in the spectrum above 100 Gc. Considerable investigation will be required to secure suitable detectors in this frequency range.

In order to achieve a sufficiently large heatsink, it is proposed that the bulk semiconductor, with ohmic contacts, be mounted directly on a metal stud as shown in Fig. 3.2. It will be desirable to have the metal-semiconductor ohmic contact with a high melting point since the melting point of GaAs is 1237°C and should not be a limiting factor.

3.4 Conclusions. Two basically different types of bulk semiconductor oscillation which have been reported in the literature have been discussed. Of the two, the Gunn Radiation Experiment has considerably more potential. The mechanism of stimulated emission of Bremsstrahlung has been proposed to explain Gunn's results. Calculations, using the theory presented by Marcuse, indicate that oscillation and the significant amount of microwave power observed by Gunn, appear to fall well within feasible ion and electron concentrations for GaAs. The additional nonlinear mixing requirement between the high frequency modes

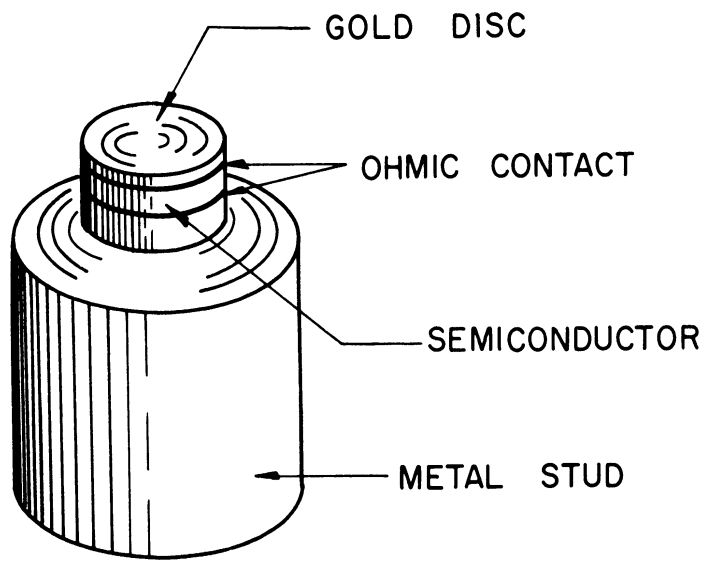
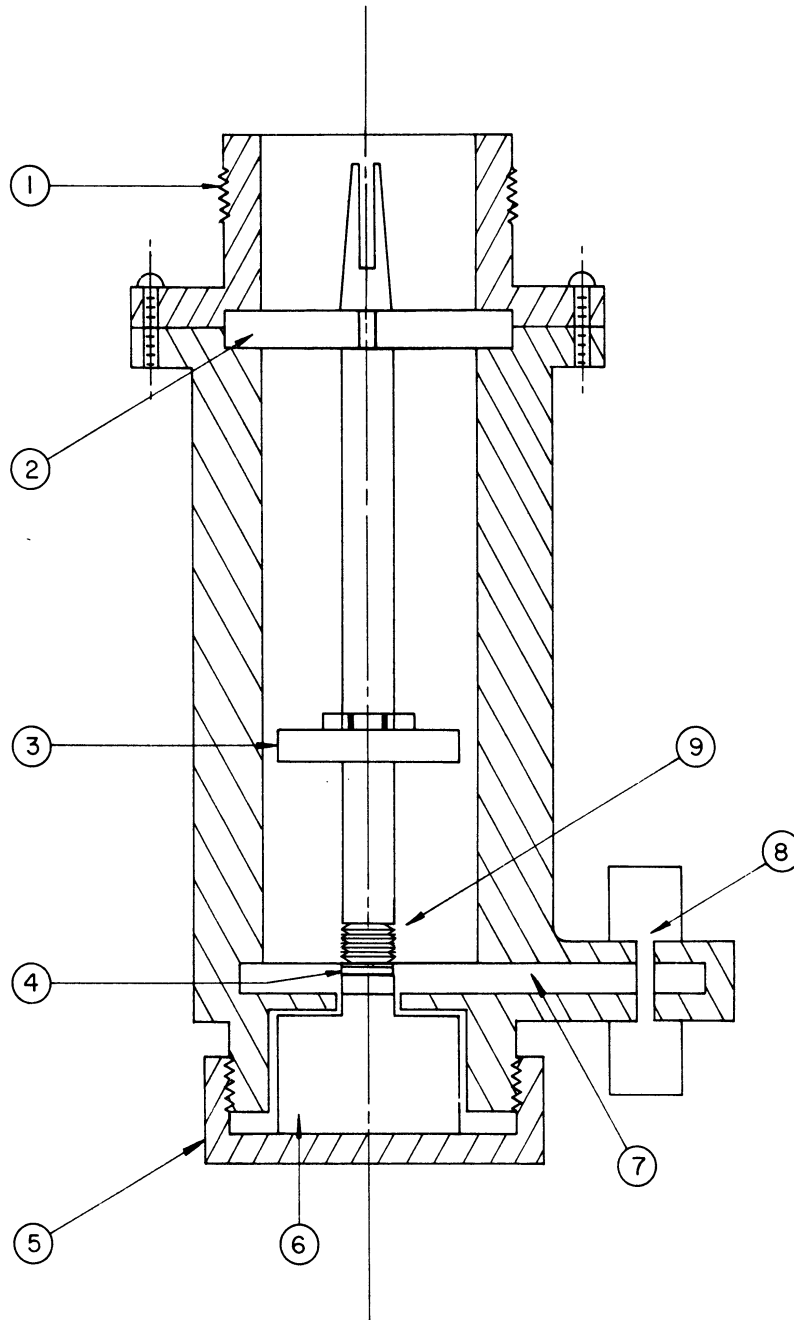


FIG. 3.1 PROPOSED MOUNT AND CONFOCAL DETECTOR.



9	CONTACTING BELLOWS
8	DETECTOR (at 2nd focal point of confocal ellipse)
7	CONFOCAL ELLIPSE
6	METAL HEAT SINK STUD
5	NUT
4	BULK SEMICONDUCTOR (at 1st focal point of confocal ellipse)
3	COAXIAL CAPACITOR FOR TUNING MICROWAVE CIRCUIT
2	REXOLITE SUPPORT
1	N-TYPE CONNECTOR

NO. PART NAME

FIG. 3.2 BULK SPECIMEN AND HEAT SINK.

to produce the observed radiation spectrum appears feasible since the strong f^5 power relationship makes on the order of one watt of power available at 1000 Gc.

3.5 Program for the Next Quarter. In the next quarter a theoretical analysis will be initiated to evaluate in more detail the mechanism of stimulated emission of Bremsstrahlung and crystal nonlinearities. Consideration must be given to optimum boundary conditions.

An experimental program will be initiated to establish the mechanism of radiation. Considerable preliminary work must be done to secure semiconductor specimens with good characteristics and ohmic contacts. In addition much work must be done to obtain good detectors of radiation in the submillimeter and low infrared spectrum. Later experiments should be directed toward determining the angular dependence along the cylindrical axis. This will be quite difficult, however, due to the small height to diameter ratio required for oscillation and radiation.

4. Traveling-Wave Phonon Interactions (J. E. Rowe, C. Yeh)

4.1 Introduction. Traveling-wave phonon interactions in bulk semiconductor materials may be conveniently described by the coupling or overlapping of the electron wave functions and the phonon eigenstates for lattice vibrations. The longitudinal acoustical vibrations in a crystal expands or compresses the lattice at various points giving rise to a change in the effective electrostatic potential acting on the electron. Such interactions result in an interchange of energy between the lattice vibrations and the electrons (drifting charge carriers) when a d-c drift field is applied in the direction of the traveling phonon wave. Acoustic gain is realized when the carrier drift velocity exceeds the acoustic wave velocity.

Theoretical investigations of phonon interactions in semiconductors were initiated by the authors some time ago and these investigations were partially supported by the Laser Systems Center of the Lear-Siegler Corporation during the past year. This theoretical work will be summarized here and the general theoretical studies will be continued.

4.2 Literature Survey

4.2.1 Fundamental Effects. The phenomena, which shall be referred to as the phonon-wave phenomena, involves one or more of the following fundamental effects:

1. The electro acoustic effect,
2. The piezoelectric effect, and
3. The magnetic acoustic effect.

4.2.2 The Electro Acoustic Effect. Parmenter¹ discusses the generation of an electric current by a longitudinal acoustic wave along a semiconductor rod. The time average of this current depends upon the acoustic power but not on the acoustic frequency. The effect is similar in nature to the thermoelectric effect and is measurable as a voltage across the ends of the rod. He attributes this effect to the deformation potential effect discussed by Shockley². Weinreich³ formulates the equations of interaction current carriers with the acoustic wave, including the case of an applied constant longitudinal electric field. Bunching of carriers in a compressional wave is discussed. The coupling to the acoustic wave by the deformation potential appears to be much weaker than the other two effects.

-
1. Parmenter, R. H., "Acousto-Electric Effects", Phys. Rev., vol. 89, p. 990; 1953.
 2. Shockley, W., Electrons and Holes in Semiconductors, D. Van Nostrand, New York; 1950.
 3. Weinreich, G., "Acousto-Dynamic Effects in Semiconductors", Phys. Rev., vol. 104, p. 320; 1956.

4.2.3 The Piezoelectric Effect. The piezoelectric effect in crystals is of course well known. Standard books such as Mason⁴ and Cady⁵ give a good account of piezoelectricity. The I.E.E.E. publications give complete standards⁶ on piezoelectric crystals with Kyame⁷ perhaps being the first one to analyze the problem of wave propagation in piezoelectric crystals. By assuming a plane wave in a piezoelectric medium, a simultaneous solution of Maxwell's field equations and Newton's law of forces yields a 5 x 5 determinantal equation. The solutions of the 5 x 5 determinant correspond to two transverse electromagnetic waves traveling at the speed of light and three acoustic waves traveling at the speed of sound. In piezoelectric materials, the electromagnetic waves will create stresses accompanied by an acoustic wave force vibrating at the speed of light. Their amplitudes are small and the effect on the electromagnetic wave is negligible. Each acoustic wave may create an electric field with transverse and longitudinal components. The transverse components are electromagnetic waves forced to travel at the velocity of sound and little effect on the acoustic wave. The longitudinal field is electrostatic in nature and has a sufficiently large effect in most piezoelectric materials to be observable. Koga⁸ et al. and Pailloux⁹ have obtained similar results.

-
4. Mason, W. P., Piezoelectric Crystal and Their Application to Ultrasonics, D. Van Nostrand, New York; 1950.
 5. Cady, W. G., Piezoelectricity, McGraw Hill, New York; 1946.
 6. "IRE Standards on Piezoelectric Crystals", Proc. IRE., vol. 37, p. 1387; 1949, vol. 46, p. 765; 1958.
 7. Kyame, J. J., "Wave Propagation in Piezoelectric Crystals", Jour. of Acoustical Soc. of America, vol. 21, p. 159; 1949.
 8. Koga, I., Azuga, M. and Yoshinaka, Y., "Theory of Plane Elastic Waves in a Piezoelectric Crystalline Medium and Determination of Elastic and Piezoelectric Constants of Quartz", Phys. Rev., vol. 109, pp. 1467-75; 1958.
 9. Pailloux, H., "Piezoelectricite Calcul Des Vitesses De Propagation", J. Phys. Radium, vol. 19, p. 525; 1958.

Strong piezoelectric effects have recently been discovered in some semiconductor materials. Hutson¹⁰ reported that ZnO and CdS have been found to be vigorous piezoelectrics with electro-mechanical coupling constants considerably exceeding that for quartz. Jaffe¹¹ et al. reported a similar finding. The photosensitive effect on the acoustical properties of CdS crystals was reported by Nine^{12,13}. Ultrasonic attenuation can be increased or decreased by illumination with white light. Correlation between the electric conductance and the ultrasonic attenuation indicates an interaction between the electrons in the conduction band and the piezoelectric field. A linear theory of the elastic wave propagation in piezoelectric semiconductors was developed by Hutson and White¹⁴. The effect of drift, diffusion and trapping of carriers for both extrinsic and intrinsic semiconductors is discussed. It is found that conductivity modulation sets an upper limit on strain amplitude.

Generation and detection of hypersonic waves was first reported by Jacobsen^{15,16}. By maintaining a 0.3 cm diameter, 3 cm long x-cut quartz crystal (with the long axis along the x-axis) at 20-77°K, and applying a pulse at 9400 mc/sec at one end (through a cavity) the signals are picked

-
10. Hutson, A. R., "Piezoelectricity and Conductivity in ZnO and CdS", Phys. Rev. Ltrs., vol. 4, pp. 505-507; May 14, 1960.
 11. Jaffe, H., Berlincourt, D., Krueger, H. H. A., and Shiozawa, L. R., Proceedings of the 14th Annual Symposium on Frequency Control, Fort Monmouth, New Jersey; May 31, 1960.
 12. Nine, H. D., "Photosensitive Ultrasonic Attenuation in CdS", Phys. Rev. Ltrs., vol. 4, pp. 359-361; April 1, 1960.
 13. Nine, H. D. and Truell, Rohn, "Photosensitive-Ultrasonic Properties of Cadmium Sulfide", Phys. Rev., vol. 123, pp. 799-803; August 1, 1961.
 14. Hutson, A. R. and White, D. L., "Elastic Wave Propagation in Piezoelectric Semiconductors", J.A.P., vol. 33, pp. 40-47; January, 1962.
 15. Jacobsen, E. H., "Generation and Detection of 9400 mc/sec. Hypersonic Waves", Phys. Rev. Ltrs., vol. 2, p. 249; 1959.
 16. Jacobsen, E. H., "Sources of Sound in Piezoelectric Crystals", Jour. of Acoustical Soc. of America, vol. 32, pp. 949-953; August, 1960.

up at an output cavity. No ultrasound propagation is observed above 77°K. Bömmel and Dransfeld¹⁷ studied the known phonon relaxation mechanism of acoustic absorption and performed some experiments on the excitation and attenuation of hypersonic waves in quartz. An x-cut quartz crystal with the free surface exposed to a high-frequency field can be used as a transducer of hypersonic waves while the rest of the crystal body acts as a transmission line.

A rather large absorption is observed above 60°K. However, this attenuation decreases very rapidly as the temperature is lowered to only a fraction below 20°K. The absorption drops to half of its original value at a temperature where the mean free path of the thermophonons is of the order of the acoustic wavelength. Experiments with different cuts of the crystal and exciting different modes are reported. The resulting physical constants such as the acoustic velocities, attenuation coefficients, combined shear and compressional viscosities are tabulated.

4.2.4 The Magneto Acoustic Effect. The magneto acoustic effect was discussed by Kittel¹⁸. Magneto elastic coupling of magnons-spin waves and phonons in a ferromagnetic crystal can produce a large effect if the frequencies of the two fields are approximately equal. This leads to the possibility of magneto-strictive transducers at microwave frequencies. Bömmel and Dransfeld¹⁹ observed the emission of transverse hypersonic waves from a Ni-film which is deposited on a quartz surface and excited to ferromagnetic resonance. Two cavities are used--the input

-
17. Bömmel, H. E. and Dransfeld, K., "Excitation and Attenuation of Hypersonic Waves in Quartz", Phys. Rev., vol. 117, pp. 1245-1252; March 1, 1960.
 18. Kittel, C., "Interaction of Spin Waves and Ultrasonic Waves in Ferromagnetic Crystals", Phys. Rev., vol. 110, pp. 836-841; May 15, 1958.
 19. Bömmel, H. and Dransfeld, K., "Excitation of Hypersonic Waves by Ferromagnetics", Phys. Rev. Ltrs., vol. 3, pp. 83-85; July 15, 1959.

cavity is coupled magnetically to the Ni coated end of the quartz, while the output cavity is coupled electrically to the quartz. For a sound frequency of 1000 mc/sec, and a magnetic field of 6000 gauss, acoustic power of 1 mw is obtained. Denton and Spencer²⁰ discussed the magnetic transducer using Yttrium iron garnet rod (YIG) in an open-ended brass block. Microwave energy is coupled to the rod by a coaxial line terminated on the end surface of the rod by a pair of cross wires. An r-f magnetic field excites a circularly polarized wave which in turn excites a shear wave on the rod. Applying a d-c magnetic field parallel to the axis of the rod and adjusting the bias for ferromagnetic resonance, acoustic energy travels along the length of the rod and can be coupled electro-magnetically to the output.

4.2.5 Related Effects. Aside from the effects mentioned in the above paragraph, a nonohmic behavior is observed both in piezoelectric semiconductors and bismuth at low temperature. Esaki^{21,22} observed the nonlinear current-voltage characteristic curves of bismuth in a strong magnetic field at a certain high electric field. He suggested making use of this effect for an r-f detector or mixer operation. Hutson²³ explains the effect of a departure from Ohm's law as simply due to the acousto-electric current mentioned above (by Weinreich's electro-acoustic effect) accompanying a large acoustic flux produced by a traveling-wave amplification process.

20. Denton, R. T. and Spencer, E. G., "Microwave Acoustics", Proc. of NEREM, Boston, Mass.; 1962.

21. Esaki, Leo, "New Phenomenon in Magnetoresistance of Bismuth at Low Temperature", Phys. Rev. Ltrs., vol. 8, pp. 4-7; January 1, 1962.

22. Esaki, Leo, "A Proposed New Bismuth Device Utilizing the Electron-Phonon Interaction", Proc. IRE, vol. 50, pp. 322-323; March 1962.

23. Hutson, A. R., "Acousto-Electric Explanation of Non-Ohmic Behavior in Piezoelectric Semiconductors and Bismuth", Phys. Rev. Ltrs., vol. 9, pp. 296-298; October 1, 1962.

4.3 Experimental Acoustic-Wave Amplifiers. Reports concerning amplification of acoustic waves first appeared in the literature in early 1961. Tucker²⁴ reported the use of maser action in ruby in amplifying microwave signals. A ruby rod (in which the spin system was inverted using a pump power at 23.3 kmc/sec) is inserted in a K-band cavity. An x-cut quartz crystal is bonded to the ruby by indium which is used as a microwave transducer. Amplification is reported when the temperature of the ruby is maintained at 1.5°K.

The first report on ultrasonic amplification that makes use of drifting carriers was reported by Hutson, McFee and White²⁵. Amplification of ultrasonic waves in a photoconductive CdS crystal is observed by applying a d-c drift field in the direction of acoustic wave propagation and with a drift carrier velocity slightly greater than the velocity of sound in the crystal. A gain of 18 db at 15 mc/sec and 38 db at 45 mc/sec in a 7 mm CdS was obtained.

Quate²⁶ developed the theory of the acoustic-wave amplifier using the coupled-mode theory developed by Pierce²⁷ and Louisell²⁸. The drifting of electrons through the piezoelectric material can be characterized by an average conduction current, wherein the velocity is proportional

-
24. Tucker, E. B., "Amplification of 9.3 kmc/sec Ultrasonic Pulses by Maser Action in Ruby", Phys. Rev. Ltrs., vol. 6, pp. 547-548; May 15, 1961.
 25. Hutson, A. R., McFee, J. H. and White, D. L., "Ultrasonic Amplification in CdS", Phys. Rev. Ltrs., vol. 7, pp. 237-239; September 15, 1961.
 26. Quate, C. F., "Coupled Mode Theory of Acoustic Wave Amplifier", Micro-wave Laboratory, Stanford University, Report No. 889; February, 1962.
 27. Pierce, J. R., "Coupling of Modes of Propagation", J.A.P., vol. 25, pp. 179-183; 1954.
 28. Louisell, W. H., Coupled Mode and Parametric Electronics; Wiley, New York; 1960.

to the electric field and an average diffusion current proportional to the gradient of the charge density in the development of coupled-mode equations. The analysis should be valid at frequencies for which the mean-free-time between collisions is small compared with an r-f cycle and the mean-free-path between collisions is small compared to the acoustic wavelength in the crystal. For a CdS crystal at room temperature, Quate²⁶ estimated the upper frequency limit to be approximately 10^{10} cps.

White²⁹ made further calculations on the amplification or attenuation of ultrasonic waves in strongly piezoelectric semiconductors and discussed the high-frequency limit. At high frequencies, gain is reduced due to the electron diffusion process smoothing out the electron bunching necessary for amplification. The d-c power required to control the drift current also increases rapidly with frequency. It is found that pulse operation is necessary at frequencies above several megacycles per second.

4.4 Amplification Theory. The general problem of wave propagation in anisotropic piezoelectric materials is a complex one and leads to a fifth degree secular equation. The five coupled system waves are made up of two transverse electromagnetic waves and three acoustic waves. In a piezoelectric material, each transverse electromagnetic wave creates stresses in the material which are accompanied by an acoustic wave forced to vibrate at the speed of light. Its amplitude is small and thus its effect on the electromagnetic wave is negligible. Each acoustic wave creates an electric field with transverse and longitudinal components. The transverse component corresponds to an electromagnetic wave forced to travel at the velocity of sound. Its effect on the acoustic wave

29. White, D. L., "Amplification of Ultrasonic Waves in Piezoelectric Semiconductors", J.A.P., vol. 33, pp. 2547-2554; August, 1962.

is again small. However, the longitudinal component is electrostatic in nature and therefore couples to charge carriers in the medium and markedly changes the acoustic wave propagation constants. The analysis given here somewhat follows along the lines of those by Hutson-White and Quate. Both longitudinal and shear excitations are considered and new gain expressions are developed.

In general wave propagation and interaction studies one must begin with the piezoelectric stress tensor which relates the applied field to the internal strains. The ultrasonic stress waves produce polarizations of the form

$$p_i = e_{ijk} T_{jk} , \quad (4.1)$$

where i,j,k = the various crystal axes,

T_{jk} = components of the stress, and

e_{ijk} = piezoelectric tensor.

Cadmium sulfide and zinc oxide are of hexagonal symmetry and if the axis of symmetry is taken along the optical axis (c- or z-axis), then the components of e_{ijk} are

$$e_{113} = e_{223} ,$$

$$e_{322} = e_{311} ,$$

$$e_{333} ,$$

all the rest being zero.

In each case the objective is to determine under which orientation with respect to the crystal a traveling acoustic wave produces a polarization in the direction of propagation. Consider longitudinal and transverse (shear) waves traveling parallel and perpendicular to the

hexagonal axis. An examination of Eq. 4.1 indicates that longitudinal polarizations are produced only when there is a longitudinal wave parallel to the hexagonal axis, such that

$$\begin{aligned} T_{jk} &= T_{33} \\ p_i &= p_3 \end{aligned} ,$$

and a shear wave perpendicular to the hexagonal axis, so that

$$\begin{aligned} T_{jk} &= T_{32} \quad , \\ p_i &= p_2 \quad , \end{aligned}$$

or

$$\begin{aligned} T_{jk} &= T_{13} \quad , \\ p_i &= p_1 \quad . \end{aligned}$$

A perfectly general analysis must consider both the acoustical and optical modes and therefore a discrete lattice model. In order to avoid the use of quantum mechanics for the present a continuous lattice model will be assumed. This corresponds to a low-frequency model where the frequency is sufficiently low so that the acoustic wave period is much longer than the time between electron lattice collisions. Furthermore, only one charge carrier species will be considered.

For simplicity reasons the three-dimensional model discussed above is abandoned and a one-dimensional model is assumed in which the acoustic wave propagates in the z-direction and the charge carriers drift in the same direction.

The strain and displacement are related by

$$S = \frac{\partial y}{\partial z} \tag{4.2}$$

and the stress and displacement are related by

$$\frac{\partial T}{\partial z} = \rho_m \frac{\partial^2 y}{\partial t^2} , \quad (4.3)$$

where ρ_m denotes the medium mass density and y denotes the displacement.

In a one-dimensional model the strain S produces an electric field in the z -direction and the piezoelectric constant can be given by "e" without subscript. Thus the equations of state are

$$T = cS - eE \quad (4.4)$$

and

$$D = eS + \epsilon E , \quad (4.5)$$

where c = the elastic constant for constant E ,

ϵ = the dielectric permittivity for constant S .

The following equations may be written in the light of the small-amplitude assumption:

$$\rho = \rho_0 + \rho_1 , \quad \rho_1 \ll \rho_0 , \quad (4.6)$$

$$u = u_0 + u_1 , \quad u_1 \ll u_0 , \quad (4.7)$$

$$E = E_D + E_1 , \quad E_1 \ll E_D , \quad (4.8)$$

where $\rho_0 \triangleq$ average density of the charge carriers,

$u_0 \triangleq$ drift velocity,

$E_D \triangleq$ external d-c drift field

and ρ_1 , u_1 , E_1 are first-order perturbation quantities. Assume also that all perturbations vary as $e^{j(\omega t - kz)}$, where $k = \omega/v$ is the phase constant of the acoustic wave, and $v = dy/dt$ is the velocity of the acoustic wave.

Poisson's equation and the r-f current density are defined as

$$\frac{\partial D}{\partial z} = -\rho_1 \quad (4.9)$$

and

$$\begin{aligned}
 J_1 &= u_0 \rho_1 + \rho_0 u_1 - \hat{D} \frac{\partial \rho_1}{\partial z} \\
 &= u_0 \rho_1 + \rho_0 u_1 - \mu \frac{kT}{q} \frac{\partial \rho_1}{\partial z} .
 \end{aligned} \tag{4.10}$$

The first term on the right-hand side of Eq. 4.10 can be identified as the convection current density, the second term as the conduction current density which is proportional to E_1 as $u_1 = \mu E_1$, where μ is the mobility of the carrier. The last term can be identified as the diffusion current density with $\hat{D} = \mu(kT/q)$ as the diffusion constant. Following Hutson and White²⁵, it is convenient to define characteristic frequencies as

$$\begin{aligned}
 \omega_c &\triangleq \frac{\mu \rho_0}{\epsilon} \quad (\text{conductivity frequency}) , \\
 \omega_D &\triangleq \frac{qu_0^2}{\mu kT} \quad (\text{diffusion frequency}) .
 \end{aligned} \tag{4.11}$$

Equation 4.10 is now rewritten as

$$J_1 = \epsilon \omega_c E_1 + u_0 \rho_1 - \frac{u_0^2}{\omega_D} \frac{\partial \rho_1}{\partial z} . \tag{4.12}$$

The continuity equation in a one-dimensional case is

$$\frac{\partial J_1}{\partial z} + \frac{\partial \rho_1}{\partial t} = 0 . \tag{4.13}$$

Combining Eqs. 4.9, 4.12 and 4.13 yields

$$\frac{\partial^2 D_1}{\partial z \partial t} = \epsilon \omega_c \frac{\partial E_1}{\partial z} - u_0 \frac{\partial^2 D_1}{\partial z^2} + \frac{u_0^2}{\omega_D} \frac{\partial^3 D_1}{\partial z^3} . \tag{4.14}$$

Applying the exponential operator and solving for D_1 , it is found that

$$D_1 = - \frac{j\epsilon \left(\frac{\omega_c}{\omega} \right) E_1}{1 - \frac{u_0}{v} - j \left(\frac{u_0}{v} \right)^2 \frac{\omega}{\omega_D}} . \quad (4.15)$$

Now with a knowledge of E_1 and D_1 , T and S can be found from the equations of state as

$$T = c' S , \quad (4.16)$$

where

$$c' = c \left[1 + \frac{e^2}{c\epsilon} \left(\frac{1 - \frac{u_0}{v} - j \left(\frac{u_0}{v} \right)^2 \frac{\omega}{\omega_D}}{1 - \frac{u_0}{v} - j \left(\frac{u_0}{v} \right)^2 \frac{\omega}{\omega_D} + j \frac{\omega_c}{\omega}} \right) \right] . \quad (4.17)$$

From c' an attenuation constant can be found:

$$\begin{aligned} \alpha &= \frac{\omega}{v} c^{1/2} I_m \left(c'^{-1/2} \right) \\ &= \frac{\omega}{v_0} \frac{e^2}{2c\epsilon} \frac{\frac{\omega_c}{\gamma\omega}}{1 + \left(\frac{\omega_c}{\gamma\omega} \right)^2 \left[(1-\gamma)^2 \frac{\omega^2}{\omega_c \omega_D} - 1 \right]^2} , \end{aligned} \quad (4.18)$$

where $\gamma = 1 - u_0/v$,

$v_0 = \sqrt{c/\rho_m}$ = the unperturbed acoustic velocity.

The scale factor $e^2/c\epsilon$ is an electromechanical coupling constant which is proportional to the ratio of mechanical to electrical energy stored in the medium. It can be seen that if $u_0 > v$, i.e., if the drift velocity of the carriers is maintained at a value slightly greater than the acoustic wave velocity in the medium, α becomes negative and the attenuation constant α in Eq. 4.18 is therefore also negative. In other words, acoustic gain instead of attenuation results.

If one introduces the Debye length defined as

$$\Lambda^2 \triangleq \left[\frac{\omega^2}{\omega_c \omega_D k^2} \right] (1-\gamma)^2, \quad (4.19)$$

into Eq. 4.18 the following results:

$$\alpha = \frac{\omega}{v_0} \frac{e^2}{2c\epsilon} \frac{\frac{\omega_c}{\gamma\omega}}{1 + \left(\frac{\omega_c}{\gamma\omega} \right)^2 [k^2\Lambda^2 - 1]^2}. \quad (4.20)$$

Notice that $\omega_c/\gamma\omega$ and $k^2\Lambda^2$ always appear as individual entities. Thus if one chooses $\omega_c/\gamma\omega$ as a variable, the quantity $k^2\Lambda^2$ can be treated as a parameter. A plot of $(\alpha v_0/\omega)/(e^2/2c\epsilon)$ against $\gamma\omega/\omega_c$, using $k^2\Lambda^2 - 1$ as a parameter, results in a universal graph for the gain constant of the phonon-wave amplifier. Such a plot is shown in Fig. 4.1.

The significance of the parameter $k^2\Lambda^2$ needs further explanation. From Eq. 4.19, it can be found that

$$k^2\Lambda^2 = \frac{\omega^2}{\omega_c \omega_D} (1-\gamma)^2. \quad (4.21)$$

Since $\gamma = 1 - u_0/v$ is usually a small negative number for proper amplifier operation, then $1-\gamma \approx 1$, and $k^2\Lambda^2 \approx \omega^2/\omega_c \omega_D$. $k^2\Lambda^2$ is thus related intimately to the conductivity and diffusion frequencies of the piezoelectric material. It appears in Eq. 4.20 as $[k^2\Lambda^2 - 1]^2$, so for this discussion (for a gain constant α) it is reasonable to use $(k^2\Lambda^2 - 1)$ as a parameter. The significance of this new parameter can easily be seen from Eq. 4.20, if $(k^2\Lambda^2 - 1) = 0$ or $(k^2\Lambda^2 = 1)$,

$$\alpha = \frac{\omega}{v_0} \frac{e^2}{2c\epsilon} \frac{\omega_c}{\gamma\omega} = \frac{\omega_c}{\gamma v_0} \frac{e^2}{2c\epsilon} = \text{a constant} \quad (4.22)$$

and Eq. 4.22 appears as a straight line labeled $|k^2\Lambda^2 - 1| = 0$ in Fig. 4.1.

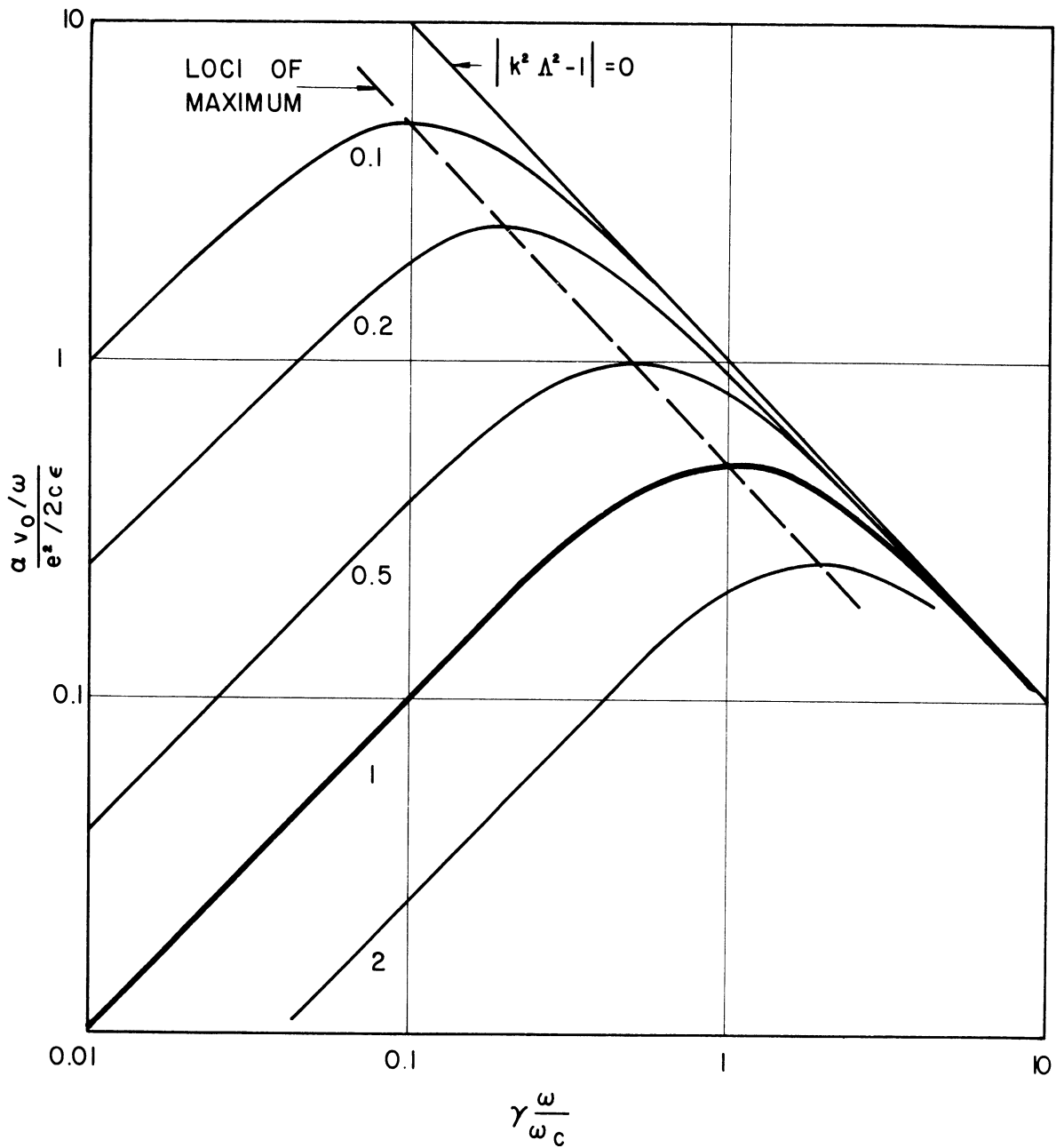


FIG. 4.1 NORMALIZED GAIN (OR ATTENUATION) $(\alpha v_0 / \omega) / (e^2 / 2c \epsilon)$ VS. FREQUENCY $\gamma(\omega / \omega_c)$ FOR VARIOUS VALUES OF THE PARAMETER $k^2 \Lambda^2 - 1$.

Equation 4.20 can be optimized to obtain the maximum gain. It is found that this occurs at $|\gamma(\omega/\omega_c)| = |(k^2\Lambda^2-1)|$ and the value of the maximum gain is

$$\alpha_m = \frac{\omega e^2}{v_o 2c\epsilon} \frac{1}{2(k^2\Lambda^2-1)} \quad (4.23)$$

Curves of the normalized α for the various values of the parameter $|k^2\Lambda^2-1|$ show a general pattern of increase with increasing $\gamma(\omega/\omega_c)$ at first and then gradually leveling off toward a maximum indicated by Eq. 4.23. From there on, the curves fall off asymptotically toward the gain curve labeled $|k^2\Lambda^2-1| = 0$. Notice that the loci of the maximum gain for various values of $|k^2\Lambda^2-1|$ follows a straight line parallel to that for $|k^2\Lambda^2-1| = 0$. This indicates that the maximum gain for various values of $|k^2\Lambda^2-1|$ is also frequency independent. $|k^2\Lambda^2-1| = 1$ is another interesting limit of operation. It corresponds to $k^2\Lambda^2 = 2$ or $k^2\Lambda^2 \ll 1$. The significance of $k^2\Lambda^2 \ll 1$ can be seen from Eq. 4.21 which indicates that $\omega_c/\omega \gg \omega/\omega_D$, and if $|\gamma(\omega/\omega_c)| = 1$, the maximum gain becomes

$$\alpha_m = \frac{\omega}{v_o} \frac{e^2}{2c\epsilon} \frac{1}{2} = \frac{\omega_c}{v_o} \frac{e^2}{2c\epsilon} \frac{1}{2\gamma} \quad (4.24)$$

Now let $N = (\omega/2\pi v_o) L = L/\lambda =$ the length of the crystal in acoustic wavelengths; then the maximum gain in db is given by

$$G_{\max.} = 27.3 \left(\frac{e^2}{2c\epsilon} \right) N \quad \text{db} \quad (4.25)$$

If $\omega/\omega_D \ll 1$, $\omega_c/\omega \ll \omega/\omega_D$ both the conduction and diffusion currents are small compared to the displacement current.

Cases corresponding to $|k^2\Lambda^2-1| > 1$ could be of interest at very high frequencies although the gain will be reduced approximately as the square of $k^2\Lambda^2-1$, and it is hoped that it can be made up if one can grow longer crystals.

To obtain high gain, it seems that $k^2\Lambda^2$ should be chosen such that

$$0 < k^2\Lambda^2 < 2$$

or

$$0 < |k^2\Lambda^2 - 1| < 1 \quad ; \quad (4.26)$$

however, due to the change of acoustic velocity at smaller values of $k^2\Lambda^2 - 1$, to be discussed in the next section, it is advisable that the operating point be kept as close to $(k^2\Lambda^2 - 1) = 1$ as possible.

4.5 The Acoustic Velocity. Equation 4.17 can also be used to derive the equation for the acoustic velocity. It can be shown easily that the acoustic velocity of propagation is given by

$$v = \frac{\text{Real } \sqrt{c'}}{\sqrt{\rho_m}} = v_o \frac{\text{Real } \sqrt{c'}}{\sqrt{c}} \quad . \quad (4.27)$$

Use of Eq. 4.17 and carrying out the indicated manipulation, one obtains

$$v = v_o \left\{ 1 + \frac{e^2}{2c\epsilon} \frac{1 + \left(\frac{1-\gamma}{\gamma}\right)^2 \frac{\omega_c}{\omega_D} \left[(1-\gamma)^2 \frac{\omega^2}{\omega_c \omega_D} - 1 \right]}{1 + \left(\frac{\omega_c}{\gamma\omega}\right)^2 \left[(1-\gamma)^2 \frac{\omega^2}{\omega_c \omega_D} - 1 \right]^2} \right\} \quad . \quad (4.28)$$

Again, let

$$k^2\Lambda^2 = (1-\gamma)^2 \frac{\omega^2}{\omega_c \omega_D}$$

and then

$$v = v_o \left[1 + \frac{e^2}{2c\epsilon} \frac{1 + \left(\frac{\omega_c}{\gamma\omega}\right)^2 k^2\Lambda^2 (k^2\Lambda^2 - 1)}{1 + \left(\frac{\omega_c}{\gamma\omega}\right)^2 [k^2\Lambda^2 - 1]^2} \right] \quad . \quad (4.29)$$

It is seen in Eq. 4.29 that $\omega_c/\gamma\omega$ appears as one variable and $k^2\Lambda^2$ the other. A plot of $(v/v_0-1)/(e^2/2c\epsilon)$ against $\gamma(\omega/\omega_c)$ with $k^2\Lambda^2$ as parameters results in a universal graph as shown in Fig. 4.2. Several interesting points can be discussed:

a. For $k^2\Lambda^2-1 = 0$ or $k^2\Lambda^2 = 1$ the acoustic velocity remains a constant throughout the frequency variation in $[\gamma(\omega/\omega_c)]$.

b. For $(k^2\Lambda^2-1) = \infty$, the velocity is again reduced to a constant value the same as in case a.

c. For $k^2\Lambda^2-1 = \mp a$, where $|a| > 0$, the equation for the acoustic velocity can be rewritten as

$$\frac{\left(\frac{v}{v_0} - 1\right)}{\frac{e^2}{2c\epsilon}} = \frac{1 + a(a+1) \left(\frac{\omega_c}{\gamma\omega}\right)^2}{1 + a^2 \left(\frac{\omega_c}{\gamma\omega}\right)^2} \quad \text{for } a > 0 \quad (4.30)$$

and

$$\frac{\left(\frac{v}{v_0} - 1\right)}{\frac{e^2}{2c\epsilon}} = \frac{1 - a(1-a) \left(\frac{\omega_c}{\gamma\omega}\right)^2}{1 + a^2 \left(\frac{\omega_c}{\gamma\omega}\right)^2} \quad \text{for } a < 0 \quad (4.31)$$

It is then possible to make the quotient negative for $a < 1$, which means that the acoustic velocity can be made slower than the unperturbed velocity of the material. It is doubtful that this will have any useful application.

For amplifier operation, it is desirable to keep the acoustic velocity as constant as possible. A range for $k^2\Lambda^2-1 = 1$ would be adequate as the range of constant v extends beyond $\gamma(\omega/\omega_c) = 1$ (and larger). A cross check with Fig. 4.1 reveals the fact that the gain constant is only moderate within the same range.

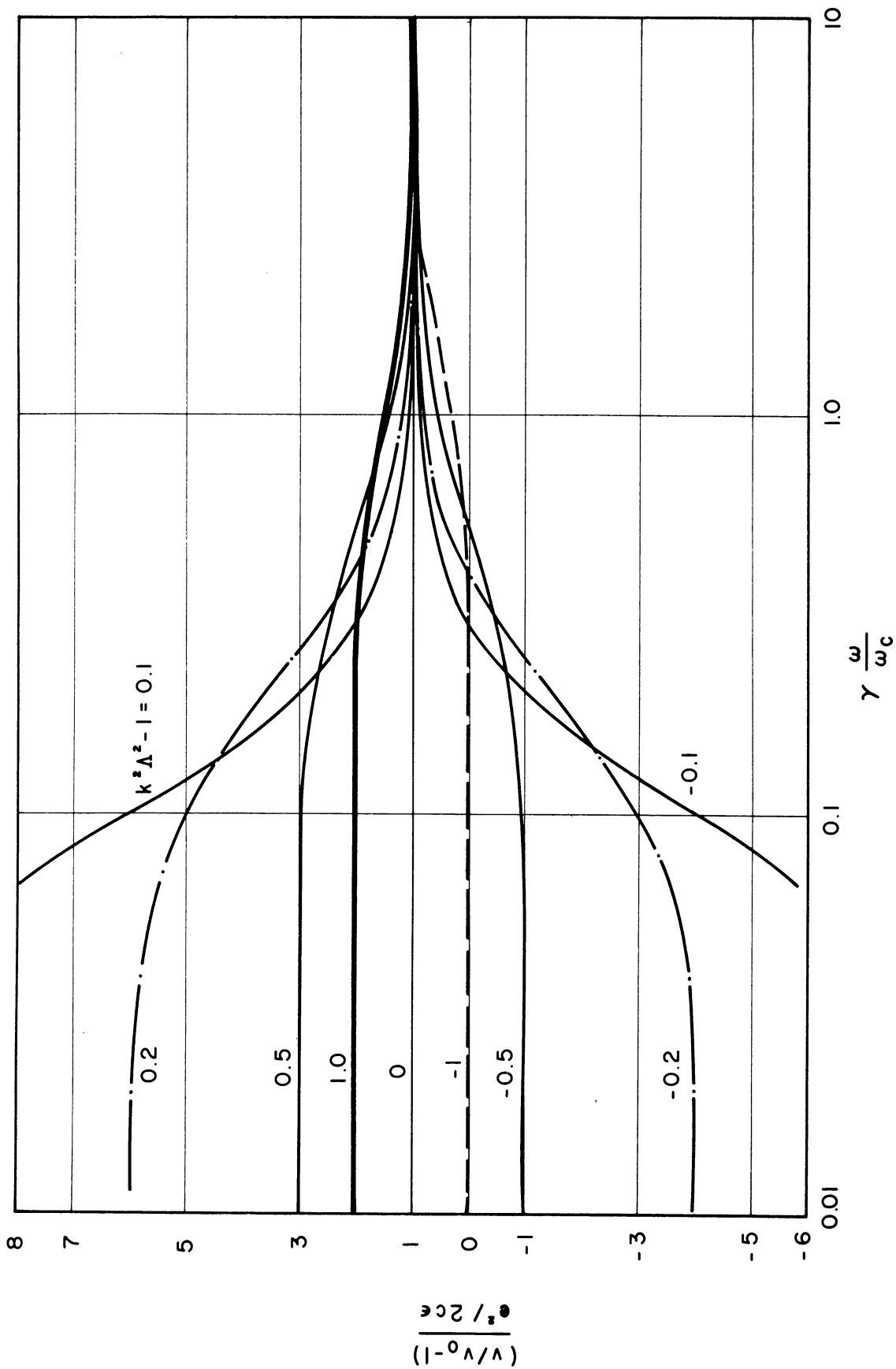


FIG. 4.2 NORMALIZED ACOUSTIC VELOCITY $[(v/v_0) - 1]/(e^2/2ce)$ VS. FREQUENCY $\gamma(\omega/\omega_c)$ FOR VARIOUS VALUES OF THE PARAMETER $k^2\Lambda^2 - 1$.

$k^2\Lambda^2 - 1 = -1$ (or $k^2\Lambda^2 = 0$) is a trivial case as it requires a conductivity or diffusion frequency of the material to be infinitely high.

For $0 < k^2\Lambda^2 - 1 < 1$, the acoustic velocity varies with $\gamma(\omega/\omega_c)$. A correlation with the gain graph reveals the fact that the higher the gain is the more rapidly and over a wider frequency range is the variation of the acoustic velocity. Thus it appears less attractive to operate an amplifier for higher gain than that obtained at $k^2\Lambda^2 - 1 = 1$.

For $|k^2\Lambda^2 - 1| > 1$, the variation of the acoustic velocity with frequency becomes less. This is in favor of operating at higher frequencies, although the gain per unit length of the crystal will be smaller necessitating longer crystals.

Gain calculations for acoustic-wave amplifiers using CdS indicate longitudinal mode gains of near 25 db/cm and for shear mode excitation 50 db/cm. It is planned to investigate the shear mode phenomena further.

4.6 Conclusions. Correlation between the gain and velocity graphs indicates the range for proper operation of an acoustic-wave amplifier. For a low frequency of operation, it is desirable to keep $k^2\Lambda^2 - 1$ close to unity. This insures near constant acoustic velocity and reasonable gain. At high frequencies, where $k^2\Lambda^2 > 1$, the velocity variation is small but the gain is reduced. To compensate for the loss of gain, a longer crystal is required for adequate total gain. The high gain per unit length characteristic of the shear mode indicates that further work on this subject is needed.

4.7 Program for the Next Quarter. It is planned that the investigations on acoustic-wave interactions will be directed toward the following areas during the next period.

- a. Shear mode gain characteristics and the excitation of shear waves.
- b. Coupling transducers for both shear and longitudinal modes.
- c. Evaluation of materials for acoustic-wave devices.
- d. Multi-stream instabilities.

<p>DDC</p> <p>The University of Michigan, Electron Physics Laboratory, Ann Arbor, Michigan. SOLID-STATE MICROWAVE RESEARCH, by D. C. Hanson, J. E. King, J. E. Rowe, C. Yeh. March, 1964, 62 pp. incl. illus. (Contract No. AF 33(657)-11587)</p> <p>The research investigations described herein relate directly to the general nature of microwave interactions in bulk solid-state materials, which is the principal objective of this broad study. The specific research tasks described in this report relate to the generation and/or amplification of coherent electromagnetic radiation in the microwave-optical regime of the spectrum.</p> <p>In particular the following three subjects are currently under study and discussed in this report. 1. General parametric phonon interactions in solids. 2. Radiation from bulk materials. 3. Traveling-wave phonon interactions. The general nature of each of these phenomena is outlined in this report and both theoretical and experimental active programs are outlined.</p>	<p>CLASSIFIED</p> <ol style="list-style-type: none"> 1. Introduction 2. Phonon Interaction in Solids 3. Radiation from Solids 4. Traveling-Wave Phonon Interaction <ol style="list-style-type: none"> I. Hanson, D. C. II. King, J. E. III. Rowe, J. E. IV. Yeh, C. <p>CLASSIFIED</p>
<p>DDC</p> <p>The University of Michigan, Electron Physics Laboratory, Ann Arbor, Michigan. SOLID-STATE MICROWAVE RESEARCH, by D. C. Hanson, J. E. King, J. E. Rowe, C. Yeh. March, 1964, 62 pp. incl. illus. (Contract No. AF 33(657)-11587)</p> <p>The research investigations described herein relate directly to the general nature of microwave interactions in bulk solid-state materials, which is the principal objective of this broad study. The specific research tasks described in this report relate to the generation and/or amplification of coherent electromagnetic radiation in the microwave-optical regime of the spectrum.</p> <p>In particular the following three subjects are currently under study and discussed in this report. 1. General parametric phonon interactions in solids. 2. Radiation from bulk materials. 3. Traveling-wave phonon interactions. The general nature of each of these phenomena is outlined in this report and both theoretical and experimental active programs are outlined.</p>	<p>CLASSIFIED</p> <ol style="list-style-type: none"> 1. Introduction 2. Phonon Interaction in Solids 3. Radiation from Solids 4. Traveling-Wave Phonon Interaction <ol style="list-style-type: none"> I. Hanson, D. C. II. King, J. E. III. Rowe, J. E. IV. Yeh, C. <p>CLASSIFIED</p>
<p>DDC</p> <p>The University of Michigan, Electron Physics Laboratory, Ann Arbor, Michigan. SOLID-STATE MICROWAVE RESEARCH, by D. C. Hanson, J. E. King, J. E. Rowe, C. Yeh. March, 1964, 62 pp. incl. illus. (Contract No. AF 33(657)-11587)</p> <p>The research investigations described herein relate directly to the general nature of microwave interactions in bulk solid-state materials, which is the principal objective of this broad study. The specific research tasks described in this report relate to the generation and/or amplification of coherent electromagnetic radiation in the microwave-optical regime of the spectrum.</p> <p>In particular the following three subjects are currently under study and discussed in this report. 1. General parametric phonon interactions in solids. 2. Radiation from bulk materials. 3. Traveling-wave phonon interactions. The general nature of each of these phenomena is outlined in this report and both theoretical and experimental active programs are outlined.</p>	<p>CLASSIFIED</p> <ol style="list-style-type: none"> 1. Introduction 2. Phonon Interaction in Solids 3. Radiation from Solids 4. Traveling-Wave Phonon Interaction <ol style="list-style-type: none"> I. Hanson, D. C. II. King, J. E. III. Rowe, J. E. IV. Yeh, C. <p>CLASSIFIED</p>
<p>DDC</p> <p>The University of Michigan, Electron Physics Laboratory, Ann Arbor, Michigan. SOLID-STATE MICROWAVE RESEARCH, by D. C. Hanson, J. E. King, J. E. Rowe, C. Yeh. March, 1964, 62 pp. incl. illus. (Contract No. AF 33(657)-11587)</p> <p>The research investigations described herein relate directly to the general nature of microwave interactions in bulk solid-state materials, which is the principal objective of this broad study. The specific research tasks described in this report relate to the generation and/or amplification of coherent electromagnetic radiation in the microwave-optical regime of the spectrum.</p> <p>In particular the following three subjects are currently under study and discussed in this report. 1. General parametric phonon interactions in solids. 2. Radiation from bulk materials. 3. Traveling-wave phonon interactions. The general nature of each of these phenomena is outlined in this report and both theoretical and experimental active programs are outlined.</p>	<p>CLASSIFIED</p> <ol style="list-style-type: none"> 1. Introduction 2. Phonon Interaction in Solids 3. Radiation from Solids 4. Traveling-Wave Phonon Interaction <ol style="list-style-type: none"> I. Hanson, D. C. II. King, J. E. III. Rowe, J. E. IV. Yeh, C. <p>CLASSIFIED</p>

<p>DDC _____</p> <p>The University of Michigan, Electron Physics Laboratory, Ann Arbor, Michigan. SOLID-STATE MICROWAVE RESEARCH, by D. C. Hanson, J. E. King, J. E. Rowe, C. Yeh. March 1964, 62 pp. incl. illus. (Contract No. AF 33(657)-11587)</p> <p>The research investigations described herein relate directly to the general nature of microwave interactions in bulk solid-state materials, which is the principal objective of this broad study. The specific research tasks described in this report relate to the generation and/or amplification of coherent electromagnetic radiation in the microwave-optical regime of the spectrum.</p> <p>In particular the following three subjects are currently under study and discussed in this report. 1. General parametric phonon interactions in solids. 2. Radiation from bulk materials. 3. Traveling-wave phonon interactions. The general nature of each of these phenomena is outlined in this report and both theoretical and experimental active programs are outlined.</p>	<p>CLASSIFIED</p> <ol style="list-style-type: none"> 1. Introduction 2. Phonon Interaction in Solids 3. Radiation from Solids 4. Traveling-Wave Phonon Interaction <ol style="list-style-type: none"> I. Hanson, D. C. II. King, J. E. III. Rowe, J. E. IV. Yeh, C. <p>CLASSIFIED</p>	<p>DDC _____</p> <p>The University of Michigan, Electron Physics Laboratory, Ann Arbor, Michigan. SOLID-STATE MICROWAVE RESEARCH, by D. C. Hanson, J. E. King, J. E. Rowe, C. Yeh. March 1964, 62 pp. incl. illus. (Contract No. AF 33(657)-11587)</p> <p>The research investigations described herein relate directly to the general nature of microwave interaction in bulk solid-state materials, which is the principal objective of this broad study. The specific research tasks described in this report relate to the generation and/or amplification of coherent electromagnetic radiation in the microwave-optical regime of the spectrum.</p> <p>In particular the following three subjects are currently under study and discussed in this report. 1. General parametric phonon interactions in solids. 2. Radiation from bulk materials. 3. Traveling-wave phonon interactions. The general nature of each of these phenomena is outlined in this report and both theoretical and experimental active programs are outlined.</p>	<p>CLASSIFIED</p> <ol style="list-style-type: none"> 1. Introduction 2. Phonon Interaction in Solids 3. Radiation from Solids 4. Traveling-Wave Phonon Interaction <ol style="list-style-type: none"> I. Hanson, D. C. II. King, J. E. III. Rowe, J. E. IV. Yeh, C. <p>CLASSIFIED</p>
<p>DDC _____</p> <p>The University of Michigan, Electron Physics Laboratory, Ann Arbor, Michigan. SOLID-STATE MICROWAVE RESEARCH, by D. C. Hanson, J. E. King, J. E. Rowe, C. Yeh. March 1964, 62 pp. incl. illus. (Contract No. AF 33(657)-11587)</p> <p>The research investigations described herein relate directly to the general nature of microwave interactions in bulk solid-state materials, which is the principal objective of this broad study. The specific research tasks described in this report relate to the generation and/or amplification of coherent electromagnetic radiation in the microwave-optical regime of the spectrum.</p> <p>In particular the following three subjects are currently under study and discussed in this report. 1. General parametric phonon interactions in solids. 2. Radiation from bulk materials. 3. Traveling-wave phonon interactions. The general nature of each of these phenomena is outlined in this report and both theoretical and experimental active programs are outlined.</p>	<p>CLASSIFIED</p> <ol style="list-style-type: none"> 1. Introduction 2. Phonon Interaction in Solids 3. Radiation from Solids 4. Traveling-Wave Phonon Interaction <ol style="list-style-type: none"> I. Hanson, D. C. II. King, J. E. III. Rowe, J. E. IV. Yeh, C. <p>CLASSIFIED</p>	<p>DDC _____</p> <p>The University of Michigan, Electron Physics Laboratory, Ann Arbor, Michigan. SOLID-STATE MICROWAVE RESEARCH, by D. C. Hanson, J. E. King, J. E. Rowe, C. Yeh. March 1964, 62 pp. incl. illus. (Contract No. AF 33(657)-11587)</p> <p>The research investigations described herein relate directly to the general nature of microwave interactions in bulk solid-state materials, which is the principal objective of this broad study. The specific research tasks described in this report relate to the generation and/or amplification of coherent electromagnetic radiation in the microwave-optical regime of the spectrum.</p> <p>In particular the following three subjects are currently under study and discussed in this report. 1. General parametric phonon interactions in solids. 2. Radiation from bulk materials. 3. Traveling-wave phonon interactions. The general nature of each of these phenomena is outlined in this report and both theoretical and experimental active programs are outlined.</p>	<p>CLASSIFIED</p> <ol style="list-style-type: none"> 1. Introduction 2. Phonon Interaction in Solids 3. Radiation from Solids 4. Traveling-Wave Phonon Interaction <ol style="list-style-type: none"> I. Hanson, D. C. II. King, J. E. III. Rowe, J. E. IV. Yeh, C. <p>CLASSIFIED</p>

